Residual mechanical and bond properties of concrete and steel after exposure to elevated temperatures: A state-of-the-art review

Author: Atiqullah Fayeq, Shanghai Jiao Tong University, School of Naval Architecture, Ocean & Civil Engineering, Department of Civil Engineering.

MA Student.

Abstract

The purpose of this is the examine Residual mechanical and bond properties of concrete and steel after exposure to elevated temperatures. This study includes analysis of different strengths on the concrete in different temperatures. The data was collected from current literature where workable values might be consistently interrelated with released compressive strength, yield strength, Bond slip, tensile strength, Flexural strength, ultimate strength, Analytical solutions. The findings of this study shows a complete inventory of concrete and steel exposure elevated temperature, respectively, which is claimed to be the difficult component of temperature evaluation under the different temperature in the engineering. Moreover, the collection of data from different papers provides deeper understanding of Residual mechanical and bond properties of concrete and steel after exposure to elevated temperatures. Insights for make buildings, and undergrounds finding out temperature due to different conditions are great importance for engineers and helping the engineers to acquire more knowledge about it. Approximations of the strengths should only be used for the purpose of measurements and design.

Keywords: Compressive strength, Tensile strength, Temperature, Flexural strength, Ultimate strength.

1. Introduction

Due to the weight of population limitation of land and boom, in the instruction to efficiently resolve transportation and housing problems, the need for high-rise houses, buildings and underground creation is increasing very quickly. Such kind of civil engineering is encountering with marvelous challenges of fire destruction during their services and building. Worldwide frequently reported such kind of fire damage in the recent years, extremely frightening property and personal safety. The main cause of suck kind of damaging is high temperature which is well known on concrete micro- and meso-structure, which carries in a widespread mechanical decline of the concrete and even negative effect on the structural level, according to bar exposure and spalling of concrete on the flames, in the circumstance of fire. Therefore, due to the significance of concrete behavior in the high temperature, and about the fire several studies have been done in the recent years, on the cementitious mixtures at the high temperature, and most related strictures have been specified and studied. Although, the main focus of this study is on the compressive strength, yield strength, bond slept and so on the author provide a complete and updated collection of papers on the relevant topic and data which are mentioned above which are examined as well. Amongst the objects of the paper, the methods currently espoused to improve explain, and find out the result on the mechanical properties of concrete at high temperature are dried as well. Meanwhile, the main points of the effect of temperature on the concrete are collected, and discussed in the paper. This study mainly focuses on the discussion on the Residual mechanical and bond properties of concrete and steel after exposure to elevated temperatures is exclusive in this investigation.

2.1 Compressive Strength

The compressive strength of concrete decreases when it is exposed to elevated temperature (see figure 1). Numerous studies are conducted to study the effects of such as the specimen size, compressive strength at room temperature, and type of aggregates on the residual strength of concrete after exposure to elevated temperatures, High temperatures affect the mechanical properties of concrete (see the detailed information in Table1).

Compressive strength is a significant characteristic property of concrete. The testing temperatures range between 21 to 871°C. the testing temperature can be increased until failure occurs. In the past, in order to perform the elevated temperature test, specimen size of 75×150 mm in the chambers were used. The strength of concrete is reduced to 80% of its original strength at 760 °C. Heat stresses will have a positive effect on the temperature range between 427 to 760 °C. The heat stress severity has less effect on the compressive strength of concrete at elevated temperatures (Abrams, 1971).

The effect of fire concerning the compressive strength of concrete, the temperature ranges between room temperature and 100 to 1200 °C. size and strength is 34 MPa. Specimens (40×40×160 mm) were tested at room temperature and 100 to 1200 °C by Yuzer Compressive strength tests were performed on the specimens after cooling them to room temperature. Changes in color were detected by using the Mansell color system. It was also observed that the values increased when the temperature was increased. (Yüzer, 2004).

The effects of elevated temperature on the compressive strength of normal strength concrete (NSC). However, the temperature ranges between 0 to1000°C compressive strength of concrete equal to 55 MPa NSC are mentioned below, the specimen would be 75×145 mm.

therefore, employed several fire laboratories have shown over there well-defined properties of concrete at elevated temperatures. Meanwhile, the computer program could have carried out the

effect of fire resistance for each value and observable parameters such as load, strength and the depth cross-section of concrete (V.K.R. Kodur, 2004).

Compressive strength generally remains constant in the temperatures range 20 to 400 °C. It is significantly affected in the range 400 to 600 °C. However, the original compressive strength maybe until heat could be lost within 600 to 800 °C. as well as, the effect of size specimens 100×100×400 mm with increase in aggregate size. The residual compressive strength of concrete is substantially affected by the cooling regimes. Water spraying after 30 min can affect the compressive strength and residual compressive strength is larger than original strength at chamber temperature (Gai-Fei Peng, 2008).

When the temperature is above 600 to 800°C, compressive strength was reduced by 45% and 23%, respectively for specimens' sizes of 100×100×200 mm having compressive strength of 32 MPa at room temperature. The compressive strength of concrete is decreased along with the stiffness. However, the compressive strength of concrete with metakaolin (MK) at elevated temperature increases the durability of concrete(C.S. Poon, 2004).

High-temperature affects the concrete crushing test concrete strength and a considerable reduction is observed in the compressive strength at 1000 °C (the maximum temperature tested). The compressive strength at room temperature was 30 MPa and the size of specimens was 100×100×400 mm. (Lau, 2006).

The initial grade of impressions for the concrete specimen could provide the contrary of up to 55% residual of compressive strength. The range of temperature starts from room temperature 20 to 800 °C, concrete up until a compressive strength of 70 MPa is mentioned as long as normal strength concrete, the size specimens 305×305 mm, in addition, the effect of developing superplasticizers in the concrete could make a distinction in the version results up to 40% in the residual of compressive strength clarify this result it could be discussed the chemicals exposure can affect the level of hydration at elevated temperatures. Therefore, the compressive strength of concrete increased with the elevated temperature (Kodur V. K., 2008).

It was a common concept that strength grade effects the compressive strength under 400°C temperature because NSC has a larger strength loss. At 600°C, the compressive strength in the NS was only 34% of the original strength. However, the influence of high-temperature ranges from chamber temperature to 800°C at the compressive strength of various cement mixture and high-strength concrete. Significantly, decreases in compressive strength are then consistently noted because maximum temperatures should be increases for all concrete mixes. High-temperature mechanical test was carried out on size cube shape 150×300 mm used the compressive strength 50 MPa by (Tao Jin, 2010).

Cooling regimes, a significant effect on the compressive strength of concrete at elevated temperature also, expanded perlite aggregate (EPA) and pumice aggregate (PA) highly influence on room temperature the temperature sustainable reductions on the compressive strength mixture is heated until about 700°C. However, lightweight aggregate produce lightweight concrete with other mixture, initially mixed with water the required for dry surface soaked for half an hour priority mixing for every mixture at 100×200 mm concrete strength 54 MPa and then height the sample has partitioned three cooling regimes, firstly furnace cooling starting from room temperature, secondly water cooling peck temperature 700°C and finally cooling regimes natural cooling, the sultry specimens at top temperature 700°C had taking outside the furnace and hold on laboratory conditions at 20 ± 2 °C (Karakoç, 2013).

Compressive strength of NSC at elevated temperature is influenced by different parameters such as water-cement ratio, aggregate-paste interface, and type of stress. Kodur (2014) made pre-dried samples at 45 and 67.5% of load stress levels were smaller liable to distortion in the right direction below load. At 22.5% preload, specimens shown no sustainable variance in strains. However, the compressive strength of concrete is slightly affected through a temperature of up till 400∘C. Additionally, Calcium hydroxide is ensuring an advantageous effect on the compressive strength at room temperature (Kodur., 2014).

Effects of type of aggregate on compressive strength of concrete at elevated temperature, however, more significantly affect the larger specimens 150×150×150 mm on the compressive strength. Also, the effect of temperature followed from the room temperature to 300 °C there is an increase from 300 to 800 °C there is a decrease and up to 800 °C using 40 MPa the strength of concrete is lost. As well as normal concrete specimens had lost all the compressive strength at temperature of 1000°C, whilst 20.5% and 21% of the compressive strength used to be left for lightweight concrete (Qianmin Ma, 2015).

The effect of residual compressive strength of concrete at the high-temperatures. conducted experiments on the identification and quantification of surface cracking of concrete heated to the various temperatures from room temperature to 1250ºC. Additionally, the quantification of the residual compressive strengths of concrete after high-temperature exposure; was using ordinary Portland cement (OPC) and coarse aggregate, 12.5mm maximum size, as well as the compressive strength 70 MPa, testing after the samples had been placed in a heating oven for one hour and according to the specifications (S. O. Osuji., 2015).

The results of the test show that the residual compressive of concrete at the temperature can be distributed into three distinct stages: firstly Initial stabilizing and regaining stage, which starts from room temperature to anywhere between350 °C and 400 °C; secondly, Strength loss limelight, which starts from anywhere between 350 °C– 400 °Cto 800 °C; finally total strength loss stage, which starts after 800 °C, where the hot-temperature compressive strength deteriorates gradually with increasing temperature.in addition, investigation the effect of compressive load and vapor stresses results in a decrease of strength at 68 MPa on the size specimens of concrete of 70.7×70.7 mm (Muhammad Abid, 2017).

The comparison has shown a significant difference in mechanical properties of NSC in the last out chamber temperature and as much as 450°C. Furthermore, compared the results of tests with present code requirement on the consequences of high-temperature on concrete strength. Meanwhile, the maximum compressive strength 50 MPa at chamber temperature shall be applied to the concrete specimen before to

heat up consistent during the heat up duration. Besides, is existed of one the other concrete prisms of different size 100×100×100 mm to 80×275×500 mm (Phan, 1998).

The compressive strength specimens developed through different concrete blends ranged between 39 and 52MPa. However, as expected the compressive strength of concrete mixtures ready in a reduction of water/cement (w/c) ratios giving higher- strength for type of aggregates. Besides, the specimen substantially decreases with an increase in temperature. This reduction has very shrill outside 800 °C. The effects of w/c ratio and kind of aggregate on damaged in weight have not discovered to be important. While the specimens have been exposed to elevated temperatures from 200 to 1200 °C for two hours. The heating degree was 20 °C /min it is also effects of elevated temperatures on the weight loss of the concrete specimens is 70×70×70 mm the temperature it was should be increased wounded were around 5% and 45% afterward exposing to 200 and 1200 °C, in addition, the effect of high temperatures. These on the strength of concrete have more noticeable for concrete mixes generated by river gravel aggregate (Arioz, O., 2007).

To investigate the different specimens for categorizing the compressive strength of NSC, the difference between the properties of NSC at elevated temperatures the strength a target 70 MPa, the control size 305×305 mm. However, factors that directly affected the mechanical experiments results at the high temperatures such as (admixtures, silica fume and fly ash) improve achievable and strength. Were compressive strength significantly influenced the type of aggregate and composition of the concrete mixture (in the temperature range between 650 to 800°C).(Kodur V. D., 2010).

While performing the mechanical compression of concrete and technique increased and curing lead to significant improvements in the compressive strength at elevated temperature. furthermore, in particular, the NSC would be more suitable for use construction due to its a good resistance to temperature. also, and investigation, the effect of fire on the behavior of concrete should be above 50 MPa of concrete includes the examination conducted the effect of specimen size 100×200 mm is important on the comprehensive efficiency of NSC under fire. whole enlarging the size of the specimen may result in a relatively lesser rate of strength loss. were used the temperatures for testing from 20, 200- 800 to 1000 °C for NSC (Shah, 2019).

The temperature of compressive strength has been proposed for the concrete below elevated temperature. Furthermore, the compressive strength model suggested for various aggregate of concrete at elevated temperatures. Meanwhile, it must be appropriate to evaluate the compressive strength of concrete at elevated temperature and could be carried out on the software program for additional analysis of concrete at elevated temperatures (Samson Ezekiel, 2013).

The compressive strength of concrete after high-temperature is significant for the appraisal and repair of concrete structures after a fire, was the compressing test shown with size specimens of 70.7 × 70.7 × 70.7 mm cubes. The heating time should be set to 4 °C /min. as the temperature in the furnace attained the proposed temperature, retain the temperature for two hours to constitute the temperature of specimens homogenous. The cubic of compressive strength is the normal valuation of concrete strength grade, also, the basis of calculating the mechanical properties of concrete. Whole the specimens through each side length of 70.7 mm after various temperatures and the crucial temperature is 400 °C. as well as then exposure from 20 to 400 °C, the cubic of compressive strength is generally increased with the increasing temperature. With regard to 800 to 900°C, concrete lost its strength, so the size effects multiplier can be improving (Wenzhong Zheng, 2012).

The effect of temperature and aggregate on the compressive strength of concrete after exposure at elevated temperatures. After exposure to elevated temperature from 200 to 400◦C, He concluded that the mechanical properties will elevate greater or lesser, who can be assigned to additional hydration of cementitious materials activate with elevated temperature. However, the compressive strength initiated to reduction then exposure to 400◦C. simultaneous that elevated temperature should be dividing into two ranges effect on reactive powder concrete (RPC) strength loss, specifically, from 20 to 400◦C and 400 to 600◦C, even made an increase in the original strength. Aggregate also effect on the strength of concrete has 43 MPa grade employed. However, the size specimens 100×100×300 mm rose generally to the aimed temperature first start from 20th minute during the one-hour limit for upholding temperature, which has after maintained for the remaining 40 minutes till electric heating has turned off (Peng G. F., 2012).

The different effects for cement matrix and aggregate have results show in the compressive strength of concrete at high-temperature.108 cube specimens 70.7×70.7×70.7 mm and the compressive cube strength drops at 100 ◦C as compared to 20◦C and increases from 200 to 600◦C, while in between 200 and 800◦C it is increasing. Furthermore, the strength of concrete before 400◦C not to change but after 400◦C decreasing. It is difficult to attain absolute stability within the furnace and central temperatures at 100-400 ◦C. Also, furnace and central temperatures should be consisting of 500-800 ◦C. Moreover, the high-temperature from100 to 500° C temperatures is more effect on the strength of concrete. Also, discussed the difference between the internal and external temperatures of RPC is lager at 100-400◦C (Luo, 2012).

Experimental investigation is carried out the effect high-temperature on the degradation compressive strength of RPC, and the numerous types of aggregate were extensively the temperature test was carried out by 300 cube specimen a size of 70.7×70.7×70.7 mm, polypropylene advanced effect on the compressive strength. However, after high temperatures between 300 to 400 ◦C not obvious and after 600◦C temperature obvious. Also, considered the effect of high-temperature, size specimens and type of fiber on the concrete strength, it was found that the theory of contestant temperature after two hours test results the main temperature lower than furnace temperature around 30◦C, after 3 to 4 hours the temperature as lower change and the reduction of compressive strength after 600 to 900 ◦C the concrete strength is loss (Li, 2012).

The simplifying calculation-based includes a total decrease of the cross-section size specimens as compared to a fire-damaged area at the concrete surfaces. The depth of the damaged concrete is made equivalent to the mean depth of the 500 ◦C isotherm in the compression area of the cross-section. While the temperatures of concrete structures may be exposed to fire from tests or calculations, in addition, the foundation on the theory of concrete at temperature lager than 500 ◦C, whilst the temperature of concrete below 500 ◦C is a hypothesis to keep any strength (Eurocode 2:1992-1-2:2004, 2004).

Table 1. Summary of the research carried out on the effect of compressive strength on the residual mechanical properties of concrete.

Name	Temperatures (°C)	Compressive Strength at Room Temperatures (MPa)	Aggregates	Specimen Size (mm)
Abrams	21,93,316,427,760,871	45	Carbonate	75×150
Yuzer et al.	20,100-1200	34	Siliceous	40×40×160
Kodur et al.	0-1000	55	Siliceous	75×145
Peng et al.	20,400,600,800	43	Coarse	100×100×400
Poon et al.	20,200,600,800	32	Coarse	100×100×200
Lau et al.	25,105,200-1200	30	Coarse	100×100×400
Kodur et al.	20,100,200,500,600,800	70	Carbonate	305×305
Tao et al.	20,200-400,600,800	50	Coarse	150×300
Karakoc	20,450,500,600,700-1100	54	lightweight	100×200
Kodur	20,100,400-800	50	Siliceous	
Ma et al.	20,105,110,150,300-1200	40	Calcareous	150×150×150
Osuji et al.	24,105-1200	70	Coarse	12.5
Abid et al.	20,200,350,400-1000	68	Siliceous	70.7×70.7
Phan et al.	20,100-800,1200	50	Siliceous	100×100×100
Arioz et al.	20,110,200-1200	52	limestone	70×70×70
Kodur et al.	20,140, 200,500,600-800	70	Siliceous	305×305
Shah et al.	20,200-800,1000	50	Siliceous	100 ×200
Peng et al.	20,90,105,200-600,700	43	Fine	100×100×300
Luo et al.	20,100-800	67	Siliceous	70.7×70.7×70.7

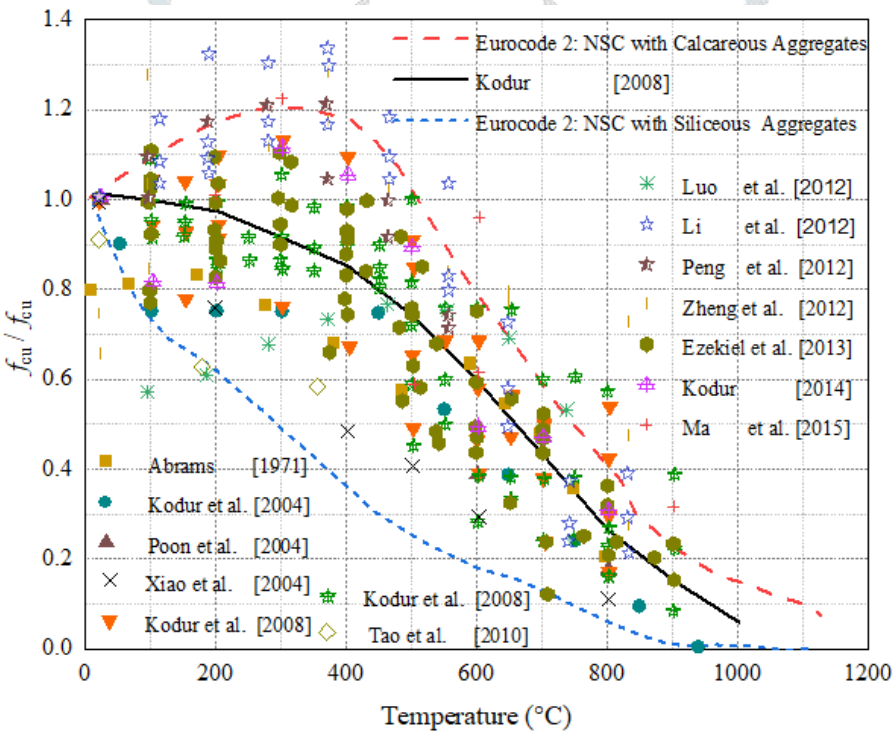

Fig.1. Relative compressive strength a function of temperature.

2.2 Compressive Stress-strain curve

The mechanical properties of concrete are generally represented through of stress-strain relationships, which are widely used for mechanical compressive strength of concrete after exposure to elevated temperature. The outline information three figures (shown in 2-4) and table 2, usually, since a brief reduction on the compressive stress-strain of concrete, the stress-strain curve reductions with increasing temperature. The strength of concrete should be having effects on stress-strain at room and elevated temperature.

The temperature has a practical effect on the compressive stress-strain response of both NSC and HSC. However, the compressive stress-strain test result has been conducted to various temperatures ranges from room temperature to 800°C, aggregate type also affects the shape of stress-strain at elevated temperature, the size specimens 150 ×300 mm the concrete strength 70 MPa widely used in various temperature (Fu-Ping Cheng, 2004).

The effects of mineral additions and test conditions on the stress-strain behavior as discussed in the concrete mixes had higher residual mechanical properties in the stressed and unstressed tests, the lager test temperature requirement up to 700°C. However, high temperatures decreased the slope on the rising branch of the stress-strain curves, unstressed test decrease would have better than within stressed test, the test

temperature starts from room temperature to 100, 200, 400 and 600°C concrete 34 MPa. The ordinary elevated temperature has 28°C/min while they were the ultimate temperature 60 min to achieve stressed tests, 40% where the target room temperature compressive strength has applied to the final room temperature compressive strength was applied in the specimens until heating. as well as the effects of metal additions and water/binder rates all the specimens for 4 days at 105°C until testing, so mostly absorbing and capillary water was expulsion. Previously 300°C, hydration also effected both stressed and unstressed tests (Fu, 2005).

The significant strain for the first of dynamic recrystallization should be obtained as a function of strain at the maximum stress. Also, the transition strain from static recrystallization to full metadynamics recrystallization must be reported to equations 1 and 2 is a function of the peak strain and stress, the maximum slope of the stress-strain curve

at the zone with a negative slope and softening mechanism must be determined. However, stress progressively reduces and great strains attain a steady-state value, the stress increases up till max value and rate, the modeled stress-strain curve up to the peak stress-strain (Solhjoo., 2007).

$$\frac{\sigma}{\sigma_p} = \left[\left(\frac{\varepsilon}{\varepsilon_p}\right) exp\left(1 - \frac{\varepsilon}{\varepsilon_p}\right)\right]^C \quad (1)$$

$$\sigma = \sigma_s + (\sigma_p - \sigma_s) exp\left[C_1\left(\varepsilon - \frac{\varepsilon_p}{2} - \frac{\varepsilon^2}{2\alpha_p}\right)\right] \quad (2)$$

Where, C is constant, σ_p ,ε_p and σ_s is the maximum stress, strain and steady-state stress respectively.

The stress-strain relationship between uniaxial and confined concrete in compression, the effect of size specimens on the uniaxial and triaxially stress-strain behavior of concrete specimens with the various appearance and also investigate the effect of aggregate size on the compression stress-strain of concrete at elevated temperature. However, normal-weight concrete cylinders the maximum compressive strengths concrete cylinders obtained strengths 56 MPa (Samani, 2012).

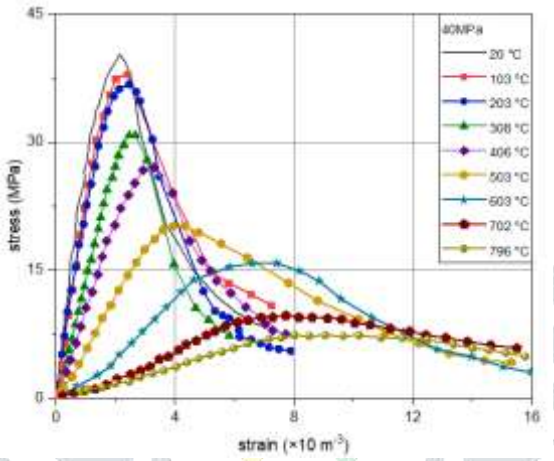

Fig.2. Experimental stress-strain curve of the concrete at different temperature

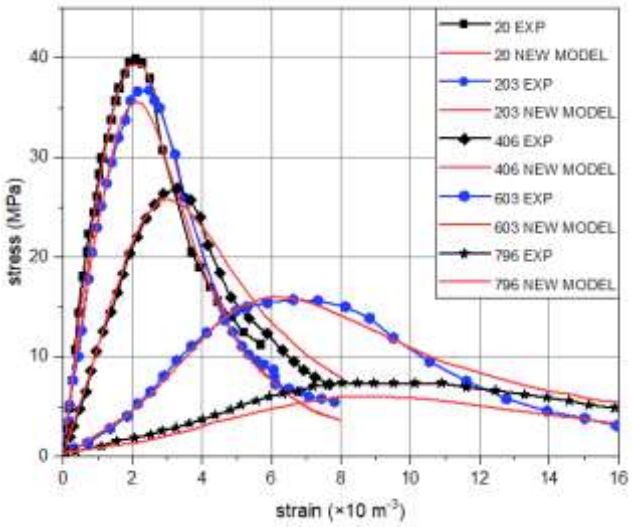

Fig.3. The stress-strain curve at a different temperature: new model vs

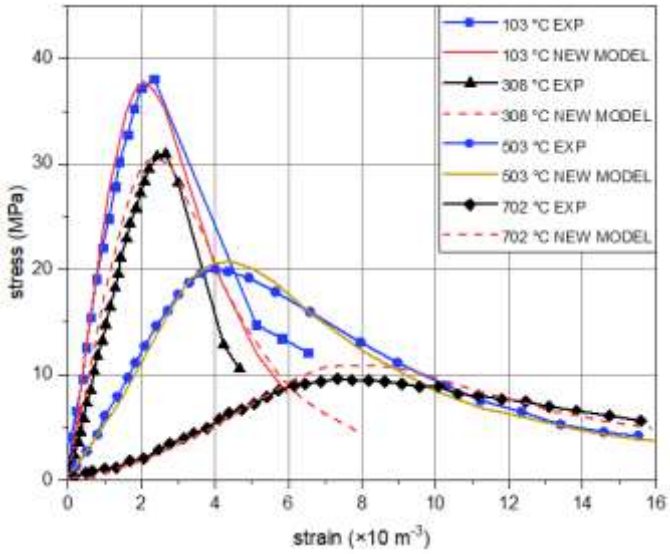

Fig.4. The stress-strain curve at a different temperature: new model vs.

2.3 Tensile strength

In numerous cases, tensile strength can have even more significance since it is an essential concept in recent engineering, especially in the field of structural engineering. Tensile strength has presented various parameters on the residual strength of concrete after exposure to elevated temperatures. Table summarized the details information of tensile strength results carried out from the previously published articles. Tensile strength of concrete generally measured through numerous procedures, such as flexural tensile, direct tension, and splitting tensile strength tests integrate mixtures of aggregate and concrete. reported that the tensile strength was conducted to determine the relationship between direct tensile strength (DTS) and Brazilian tensile strength (BTS) and to examine the validity of estimated tensile strength from other measured properties, such as the crack initiation (CI) threshold. Strength is also closely related to the stress threshold for fracture initiation in tension. Eq. (3) can determine the tensile strength of concrete.

$$K_f = \frac{2F_a K_f}{\pi D t} \qquad (3)$$

Where F_a is the applied load, D is the disk diameter, t is the disk thickness and K_f is the stress concentration factor. This factor can be calculated using Eq. (4).

$$K_f = 6 + 38\left(\frac{r}{R}\right)^2 \qquad (4)$$

Where, r is the hole radius and R is the disk radius. This type of test is now infrequently used; however, other tensile tests are still in use or are being more recently developed to overcome the difficulties with direct and indirect methods (Perras, 2014).investigated that the tensile strength of concrete can be extra sensitive to high temperatures; furthermore, the presence of PP fibers was useful for splitting tensile strength above200 °C. Well found on the experimental results, it can be reason out that the addition of 2kg PP fibers can significantly promote the residual mechanic properties of HSC during heating (Behnood, 2009). reported that the similar rends in tensile Strength loss within crease in temperature up to 800 °C. Based on their results, the relative residual tensile strength of the concrete mixture containing 10% fly ash and W/cm of 0.3 was approximately 95 %, 40%,20%, and less than 10% after subjecting to 200, 400,600, and 800 °C (Zhou, 2018). proposed that the splitting tensile strength loss esat100 °C when compared to 20 °C due to the more active role of PP fibers on splitting tensile strength when the fibers remained in the system. considering the sensitivity of tensile strength to high temperature, the ACI equations holder carefully considered for performing such as calculations at high temperatures. In general, direct tensile tests may overestimate the tensile strength of concrete. As a result, a new direct tension test method for prismatic specimens that use apply tension load to the concrete .12-16 it is the objective of this case to redevelop the direct tensile test and to determine the tensile properties of NSC at elevated temperatures. were subjected to direct tensile test from room temperature to 800°C (Lam, 2014). recommended that the direct tensile tests (DTTs) were carried out on specimens at different temperatures. There fifty-seven examples used for DTT. Moreover, were applied standards temperatures for the experiment. The samples removed from molds 72 hours after casting and were wet-cured at 23°C for 28 days. Were the tensile strengths of the natural fiber reinforced polymer(NFRP) composites increase with fiber content; up to a maximum or maximum value, the value will then drop. However, Young's modulus of the natural fiber reinforced polymer composites increases with increasing fiber loading (Ku, 2011). studied the tensile strength, and Young's modulus of composites reinforced with bleached hemp fibers increased incredibly with increasing fiber loading (Khoathane, 2008). The available literature of tensile strength is expected to decrease with

increasing recycled aggregates (RA) content. Nevertheless, it is possible to control this effect by carefully selecting the RA when producing concrete. The quality of the recycled concrete aggregate will generally vary depending on the properties of concrete. Change between the results from differences aggregate quality, aggregate size and texture, specific tensile strength, and uniformity. Although there is a noticeable effect on the 28-day tensile strength when using fly ash, it appears to have a marginal impact on tensile strength development (Silva, 2015). in their study, to achieve the under fire conditions, TS can be even more crucial in cases where fire-induced spalling occurs in a concrete structural member. The TS of concrete is generally measured through flexural tensile, direct tension, and splitting TSTs. Testing cylinder or prism specimens measure the DTS by applying axial tensile load in a suitable test machine until the specimen breaks in direct tension. The direct tension test is less reliable, as the specimen-holding devices (grips) introduce secondary stresses, leading to unreliable strength data. In the splitting tensile test, almost all the reported studies are on the residual tensile strength of concrete, which is representative of concrete cooled after exposure to fire. This remaining tensile strength data cannot be applicable for predicting fire-induced spalling because spalling occurs under hot (fire) conditions. For realistic spalling predictions, the splitting tensile strength corresponding to a hot condition required. The variation of tensile strength with temperature $(f_{t'}, T)$ can be related through a coefficient β_T, representing the ratio of the splitting tensile strength at the target temperature to the room-temperature splitting tensile strength $f_{t'}$ (Khaliq, 2011).

$$\beta_T = \frac{f_t T}{f_t} \qquad (5)$$

Showed the tensile strength increased a the 100°C. However, a significant loss was outstanding in these values for an exposure temperature of more than 100 °C. Tensile strength increased as the temperature had risen from 23 ◦C (room temperature) to 100 ◦C. However, the percentage increase in tensile strength. A significant loss tensile strength, it was noted when the temperature was increased beyond 100 ◦C. the tensile strength was reduced by only 15 % (Ahmad, 2014). reported that the tensile strength results averaged values and reduction ratios of each fire scenario. The tensile strength reduced with an increase in peak temperature, and the reductions were almost the same for all mix proportions and post-fire periods (Park, 2014). ensured that the strong influence of specimen size and increasing material deformability in the bending tests, and the excellent agreement between the thermally induced decays of tensile strength. The tensile strength in bending, on the contrary, is far too affected by the increasing ductility of the small size bent specimens (Bamonte, 2012). thus, information on the effects of tensile cracking on the thermal propagation through concrete can be ignored in structural analyses. Tensile cracking of the concrete cover is an extremely localized geometrical phenomenon that has the potential to alter the thermal propagation through a section within those localized regions. Therefore, tensile cracking will not indeed alter a material's thermal properties, yet it may still have an effect that can be described, for the purposes of numerical modeling, in terms of a local change in material properties. Tensile cracking increases the thermal propagation through the concrete, so that heat transfer is more rapid; hence the reinforcement layers will experience high temperatures more quickly than in an intact section. Tensile cracking decreases the thermal propagation through the concrete, so that heat transfer is less rapid. Hence the reinforcement layers will experience high temperatures later in a fire than a whole section. Tensile cracking does not significantly affect the thermal propagation through the concrete. The reinforcement layers will experience similar temperatures in a similar time to those experienced by a whole section. Relationship for high-temperature and tensile strength (Ervine, 2011).

Table 2. Summary of the research carried out on the effect of tensile strength on the residual mechanical properties of concrete.

References	Type of concrete	Temperature (°C)	tensile strength (MPa)	days	aggregate	Specimen size (mm)
Phan et al.	High-strength concrete	300	5	–	siliceous	–
Behnood et al.	High-strength concrete	600	0.98		fine	12.5
Lam et al.	Normal -strength concrete	800	0.753	28	coarse	5
Silva et al.	Concrete	100	20.2	28	recycled	100×100
Khaliq et al.	High-strength concrete	300	4.6	1	coarse	75×150
Ahmad et al.	Concrete	100	3.30	28	coarse	19
Park et al.	Normal -strength concrete	800	0.56	180	coarse	100×200
Bamonte et al.	light-weight concrete	500	125	–	siliceous	4.5
Grondin et al.	Concrete	500	95	28	–	160×320

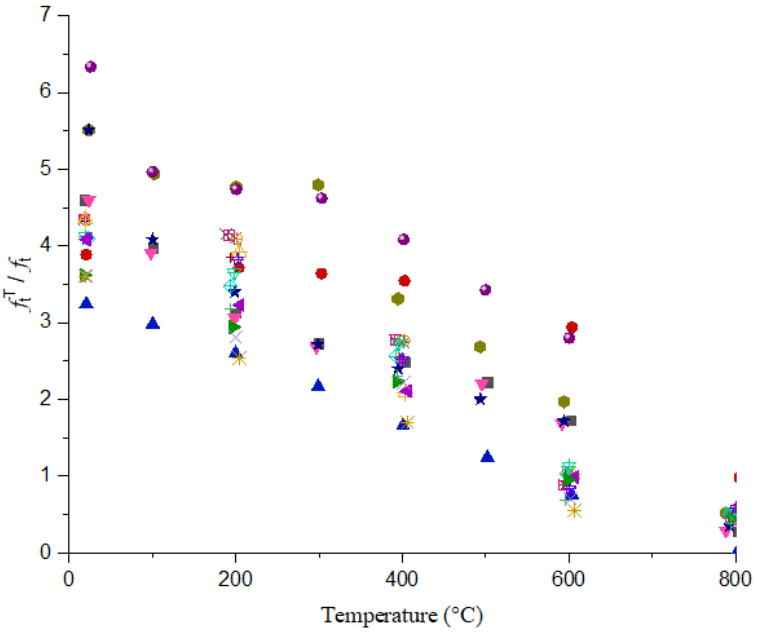

Fig. 5. Residual tensile strength of concrete at elevated temperatures.

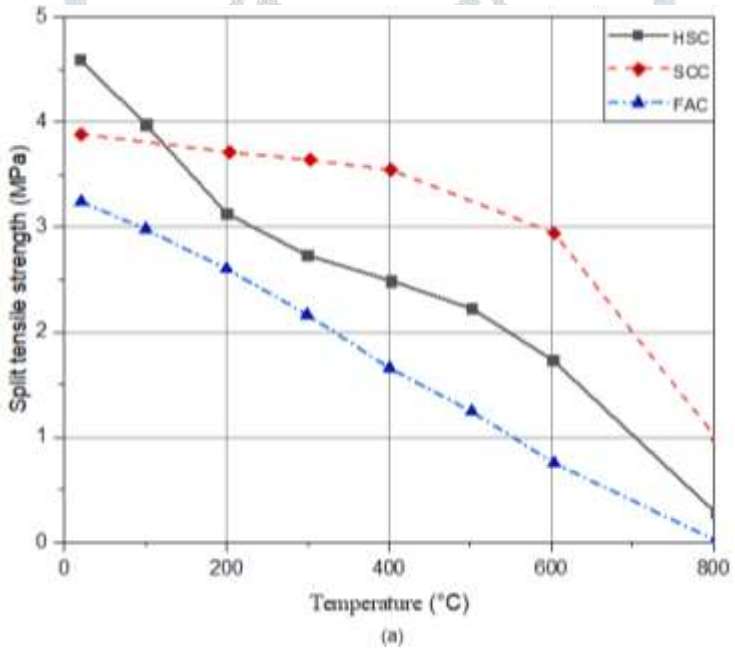

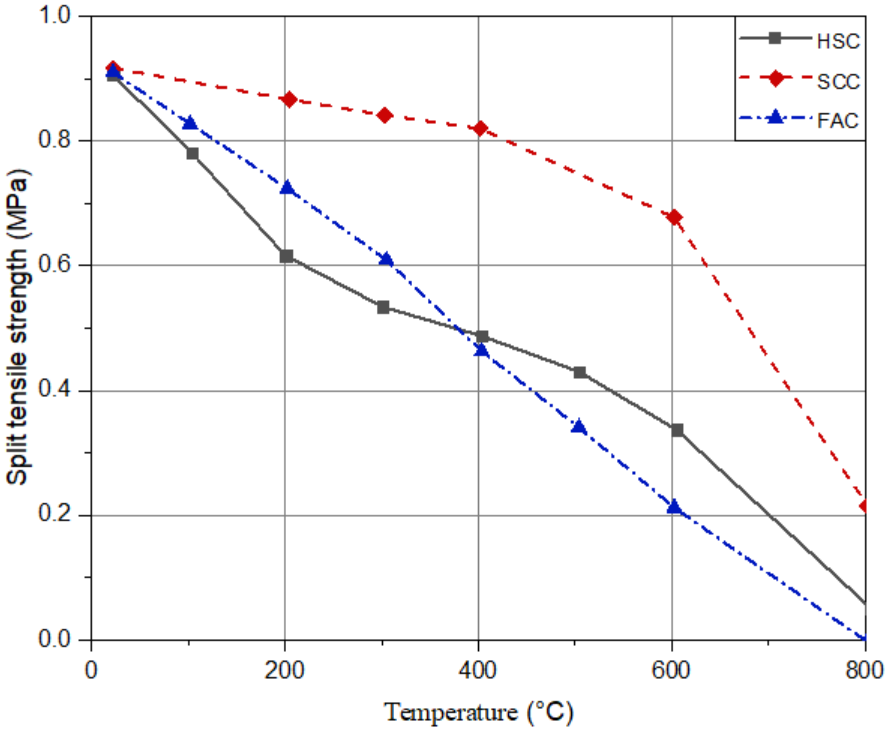

(b)

Fig. 6—Splitting tensile strengths of HSC, SCC, and FAC at various temperatures

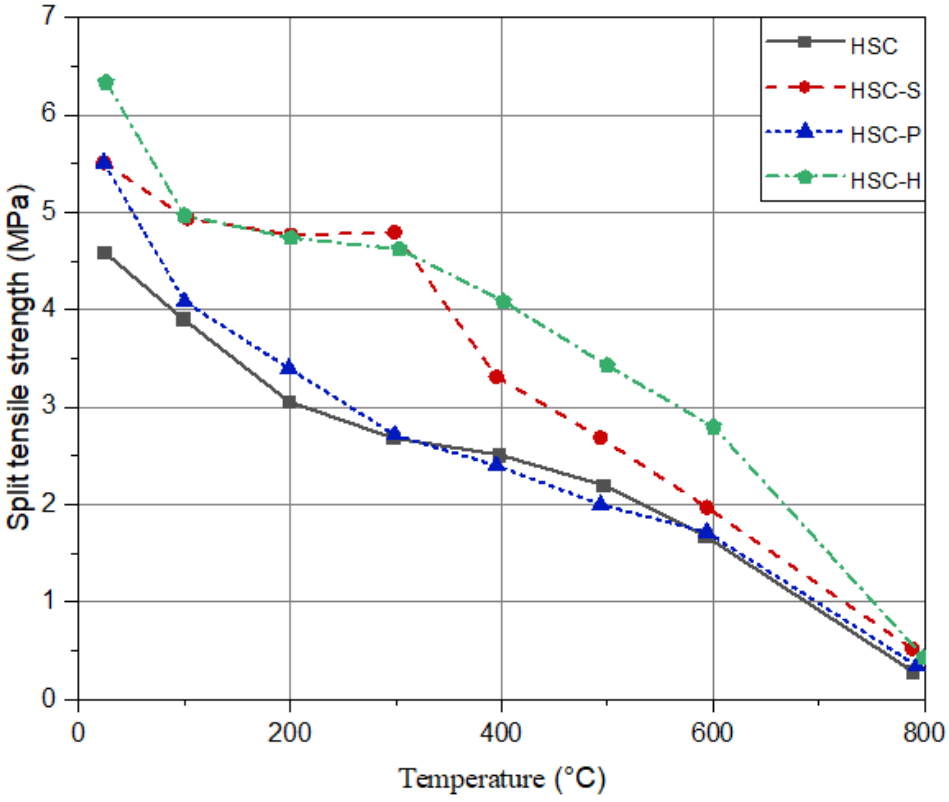

(a)

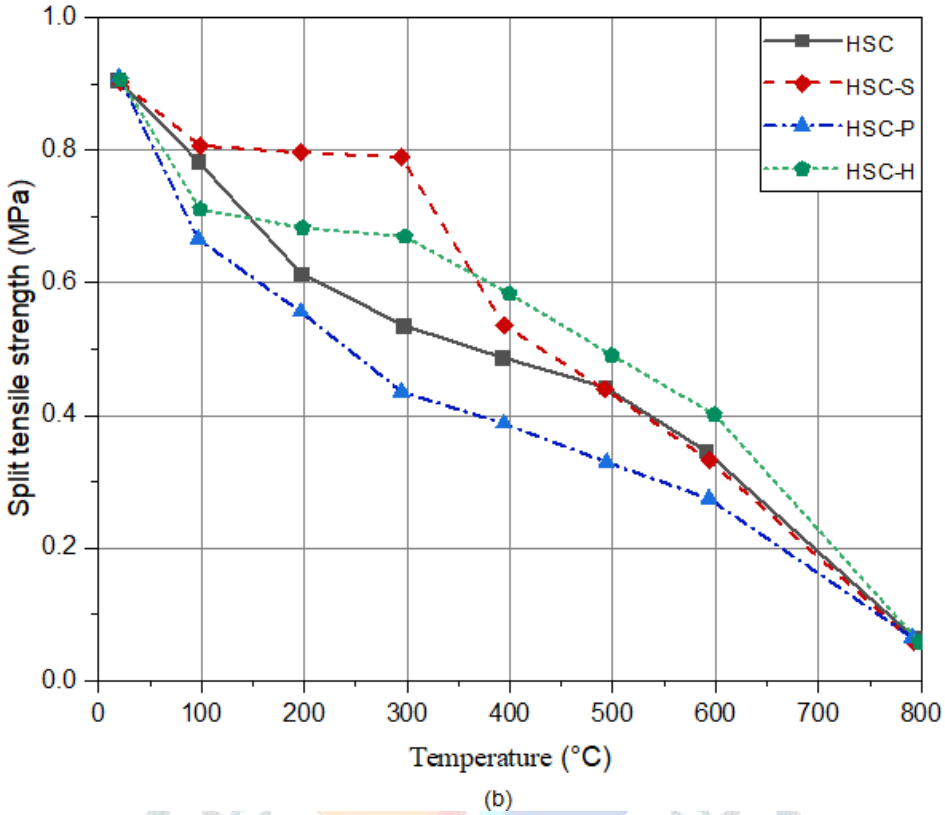

(b)

Fig. 7—Splitting tensile strengths of HSC and FRC at various

2.4 Tensile stress-strain curve

Many researchers have studied the tensile Stress-strain relationship of concrete at elevated temperatures. The details information on tensile stress-strain relationship results carried out from the previously published articles. It has been measured through numerous procedures such as direct tensile test, liner branch model, to calculate the tensile resistance of concrete at elevated temperatures and various temperatures. stated that the direct tensile test was able to estimate the complete stress-strain relationship of concrete at elevated temperatures. An entire stress-strain connection can show the complete stress-strain for all colds (Fang., 2014). reported that the tensile stress-strain relationships at elevated temperatures; the recommended formulations are presented based on well-established relationships for confined concrete at ambient temperature. A linear branch can model the uniaxial stress-strain relationship for concrete in tension until it reaches the cracking stress. The long branch can be taken equal to model the stress-strain relationship for concrete in tension. It is reported to use a linear branch until reaching the cracking stress; after cracking, an existing tension softening model was modified by accounting for the reduction in the tensile resistance of concrete and the bond resistance of the reinforcing bars (Youssef, 2007). to calculate the tensile resistance of concrete at elevated temperatures, $f_{cr\,T}$.

$$f_{cr}T = f_{cr}.(-0.000526.T + 1.01052)$$
$$20℃ \leq T \leq 400℃ \qquad (6)$$

$$f_{cr}T = f_{cr}.(-0.0025.T + 1.8)$$
$$400℃ \leq T \leq 600℃ \qquad (7)$$

$$f_{cr}T = f_{cr}.(-0.0005.T + 0.6)$$
$$600℃ \leq T \leq 1000℃ \qquad (8)$$

Where, $f_{cr\,T}$ is tensile resistance of concrete at elevated temperature (Anderberg Y, 1976).

Recommended the proposed mechanism, stress-strain relations for different locations in the localized fracture zone are pulled out from the total stress– displacement curves from test results of specimens with low boundary restraint and with various sizes and L/V-ratios. Good

agreement between studied and experimental total stress-strain curve implies that the proposed mechanism of the localization of deformations is realistic (Tung, 2015). Average stress-strain curves for concrete in tension, where cracking, bond, and shrinkage effects had taken into account in an integrated manner, have been computed for beams with various depths, reinforcement ratios, and rebar diameters. The thickness of layer *j* for the tensile zone as

$$t_{t,j,i} = y_{t,i}\frac{\varepsilon_{t,j} - \varepsilon_{t,j-1}}{\varepsilon_{t,i}} \qquad (10)$$

Where, $y_{t,i}$ = depths (taken positive) of the tensile zone, respectively, at the ith load increment. In (7), the subscript t refers to tensile concrete, i to the number of the load increment, and j to the layer number. Note that the layer numbers j varies from 1 to i and, the load increment number I varies from 1 to n. Since the number of layers increases with increasing load increment, the thickness of each layer decreases (Kaklauskas, 2001). show that the new design-oriented stress-strain model had proposed for concrete confined FRP wrap with fibers only or predominantly in the hoop direction based on a careful interpretation of existing test data and observations (Lam L. &., 2003). which is herein related to the FRP material tensile strength. This assumption is the basis for calculating the maximum confining pressure f_t (the confining pressure reached when the FRP ruptures) using the following equation:

$$f_t = \frac{2f_{frp}t}{d} \qquad (11)$$

Where, f_{frp} =FRP material tensile strength in the hoop direction. The confinement ratio of an FRP-confined specimen has defined as the ratio of the maximum confining pressure to the unconfined concrete strength (f_t/f_{co}'). However, experimental results show that in most cases of FRP material, tensile strength was not achieved at the rupture of FRP-confined concrete (ASTMD, 1992). to describe the ascending part of the stress-strain curve of unconfined concrete for design use:

$$\sigma_c = f_{co}' = \left[\frac{2\varepsilon_c}{\varepsilon_{co}} - \left(\frac{\varepsilon_c}{\varepsilon_{co}}\right)^2\right] \qquad (12)$$

Where, σ_c and ε_c are the axial stress and strain, respectively, and ε_{co} is the axial strain at the peak stress of concrete (BS 8110. Structural Use of Concrete, 1997; ENV, 1991). It is often observed that the existing design-oriented stress-strain models for The experiment results showed the effects of the strain measurement methods on the stress-strain curves. In practice, it will indicate that the stress-strain curves predicted by FEM agree well with those measured experimentally for strains determined from the crosshead displacements (Zhao, 2009).

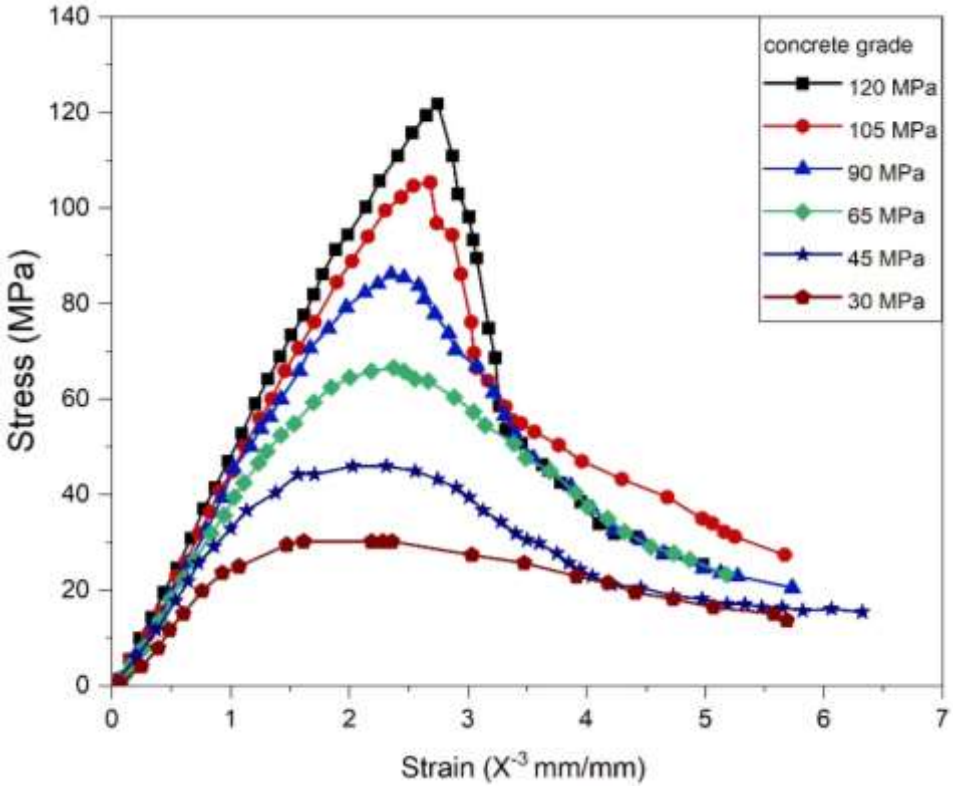

Fig.8. Typical stress-strain curve for Different Grade of Concrete.

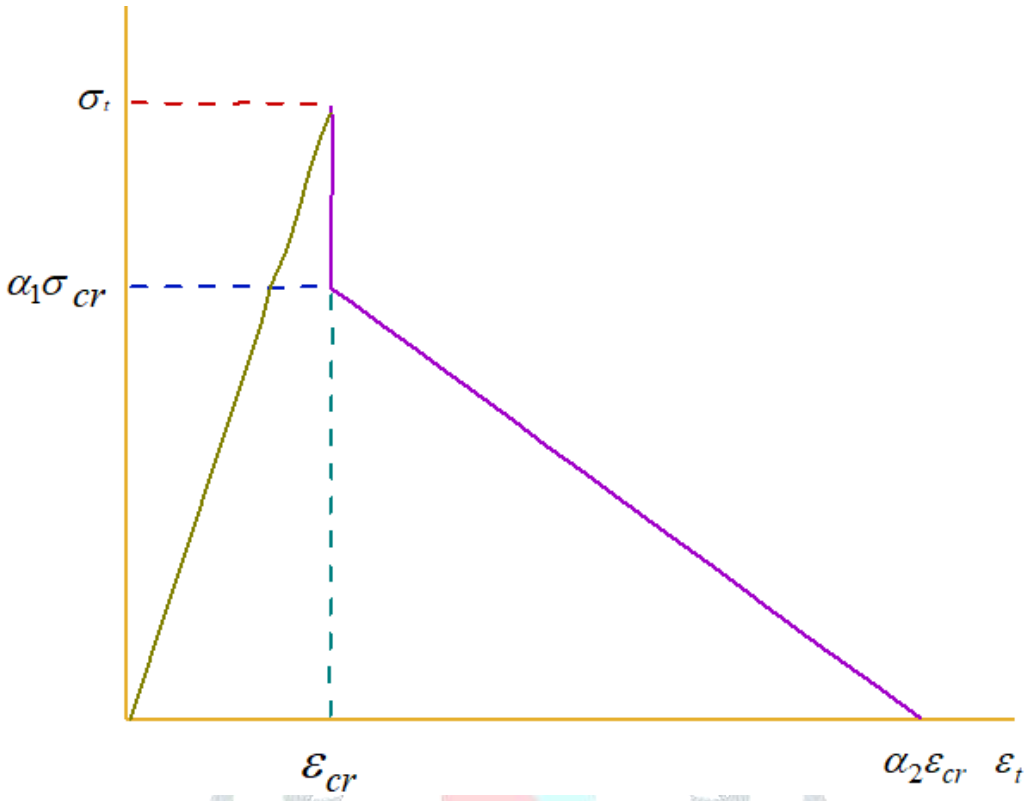

Fig. 9. Average Stress-Strain Relationship for Concrete.

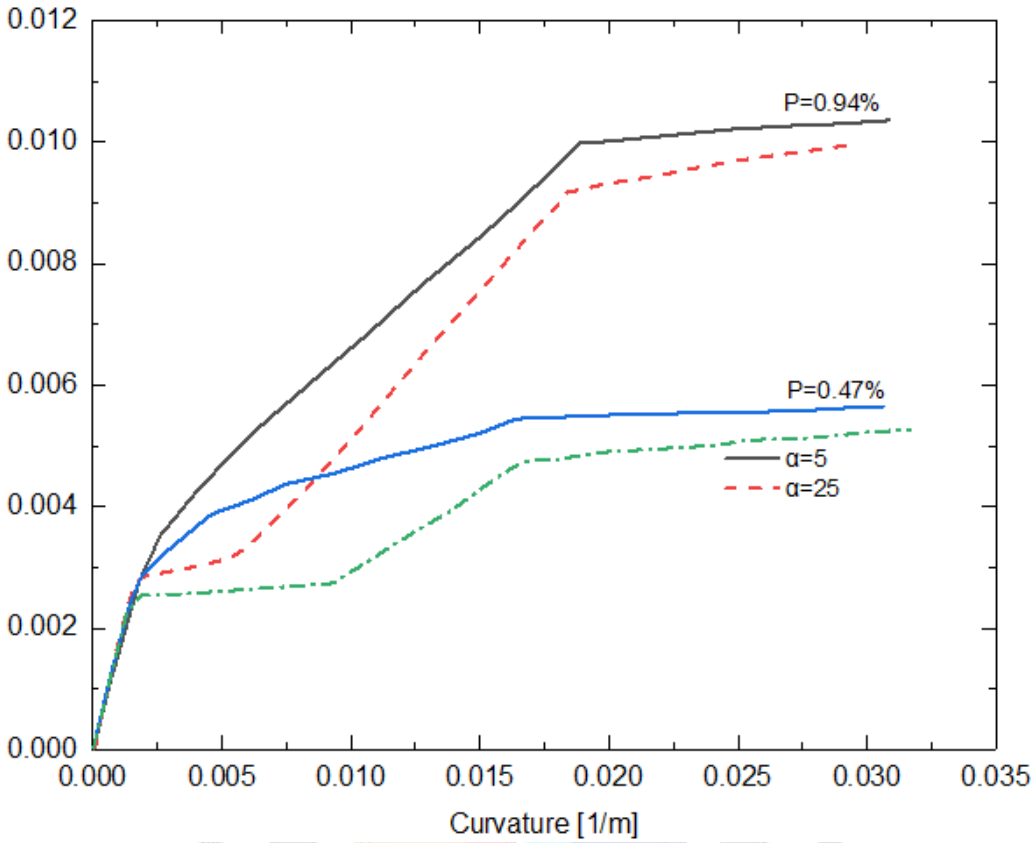

Fig. 10. Influence of Stress-Strain Relationship for Tensile Concrete on Curvature of Reinforced Concrete Members.

2.5. Flexural strength

In cases of flexural strength (FS), they are generally used on the tensile strength of concrete. The FS of concrete identifies the amount of stress and forces an unreinforced concrete and structure members. The FS has reported various parameters on the residual strength of concrete after exposure to the elevated temperatures. Table 4 summarizes the details of the FS test results from different published articles. Where some parameters recommended, such that it resists any bending failures, exposure to elevated temperature, silica fume (SF) ordinary micro-concrete (OMC), and micro-high performance (HPMC) exposed to a high temperature, cooled in water, cooled in air. ISO standard method, Lightweight foamed concrete (LWFC), different levels of strength, granite Aggregate (GA), and recycled brick aggregate (RBA) concrete with temperatures and relative humidity (RH) and latex-modified concrete (LMC). Investigated that the silica fume seemed to have a pronounced effect on FS in comparison with splitting tensile strength. For FSs, even very high percentages of silica fume significantly improved the strength. Also, it had found that there was a steady increase in the FS with an increase in the silica fume replacement percentage (Siddique, 2011; Köksal, 2008)the results indicated that the FS of ordinary micro-concrete (OMC) and micro-high performance (HPMC) exposed to a high temperature, then cooled in water, are less than those cooled in air. It is apparent that strength losses of OMC cooled in water compared to OMC cooled in the air are more than the losses of HPMC. HPMC exposed to high temperature, and FS decreases with the increase of temperature. Such a decrease is more significant in those cooled in water (Husem, 2006). The study examined the FS of concrete is generally used to evaluate its capacity in resistance of bending moment. After elevated temperatures, Polypropylene (PP) fibers can remarkably improve the FS of HPC compared with PP fibers. The FS mainly because the PP fibers can restore their tensile strength after cooling down. These PP fibers will contribute to the improvement of the FS of HPC after elevated temperatures (Xiao J. X., 2018).have been reported the FS [after 24 hands after aging in water/saliva/ethanol] and FS and fracture toughness, where standard deviation score (SDS) had calculated by dividing the raw values of the corresponding in vitro outcome by a robust estimate of their standard deviation after subtraction of their median. It is essential, as the results of tests on physical parameters like FS can vary from test institute to test institute even if the ISO standard method has

been applicable (Heintze, 2017) reported that the FSs of the compomers Dyract (DY), and Compoglass (CO) were below 80MPa; therefore, they did not meet the limit of ISO 4049 for occlusal fillings. Only Solitaire (SO), and Admira (AD) revealed significant decreases in the FS after thermocycling (Janda, 2006). recommended that the exposure to elevated temperature also affects the FS of concrete. Exposure to an elevated temperature considerably decreased in all the tested types of concrete. the relationship among the strengthen changes after exposure to an elevated temperature approximating fire condition (Drzymała, 2017). studied the presence of the fibers increase the FS of Lightweight foamed concrete (LWFC), but is also useful in reducing the drying shrinkage phenomena (Falliano, 2019). noted that the flexural tensile strength increase under confinement at a different level of strength, and the increase in flexural tensile strength decreases with the increase of the level of concrete strength under the confining condition of the concrete. The flexural tensile strength of concrete is an essential parameter for designing the flexure members. The confining conditions and age of concrete will influence the mechanical properties of concrete, including its flexural tensile strength (Ahmed, 2016). investigated that the residual flexural strength of both granite Aggregate (GA) and recycled brick aggregate (RBA) concrete with temperatures. The residual flexural strength at any temperature is said.as the percentage of the flexural strength of respective concrete at room temperature. The flexural strength decreased with the increase in temperature in both GA and RBA concretes at all temperatures (Rekha, 2016)studied that the highest flexural has gained with the addition of 3%, a further increase in fiber content decreased the strength. Therefore, the optimum dosage of steel fibers was determined to be 3%, although the flexural strengths are still higher at 5% reinforcement compared to the controlled sample, the increase in flexural strength of concrete (Oad, 2018).

Table 4. Summary of the research carried out on the effect of flexural strength on the residual mechanical properties of concrete.

References	Type of concrete	Temperature (°C)	tensile strength (MPa)	days	aggregate	Specimen size (mm)
Siddique et al.	high-performance concrete	2000	54	28	different	30 × 260
Köksal et al.	high-strength concrete	–	250kN	28	Coarse	150 ×150 ×500
Husem et al.	high-performance concrete	1000	2.8	28	limestone	40 × 40 × 160
Heintze et al.	Reinforced Concrete	55	80			16
Janda et al.	Reinforced Concrete	55	80	28		50 × 0.2 × 0.2
Drzymała et al.	high-performance concrete	600	5	28	basalt	100 × 150
Falliano et al.	fiber-reinforced concrete	30	0.2	28		40 × 40 × 160
Ahmed et al.	Plain- Concrete	–	85	28	Fine	150 ×150 ×750
Rekha et al.	Concrete	1000	–	28	Granit	100 ×100 ×500
Oad et al.	Fiber Reinforced Concrete	–	6.16	28	Fine	300×150
Kumar et al.	Fiber Reinforced Concrete	21	7	28	Coarse	0.25 ×0.25 ×19

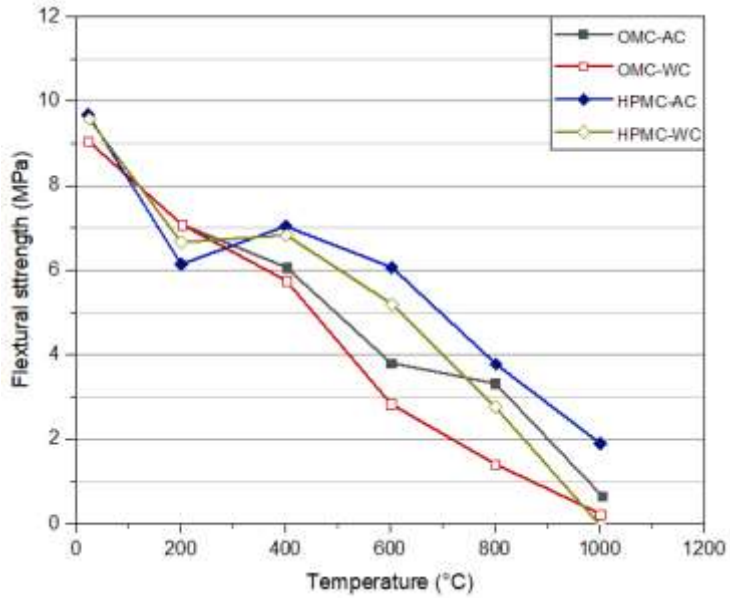

Fig.11. variation of flexural strength with temperature.

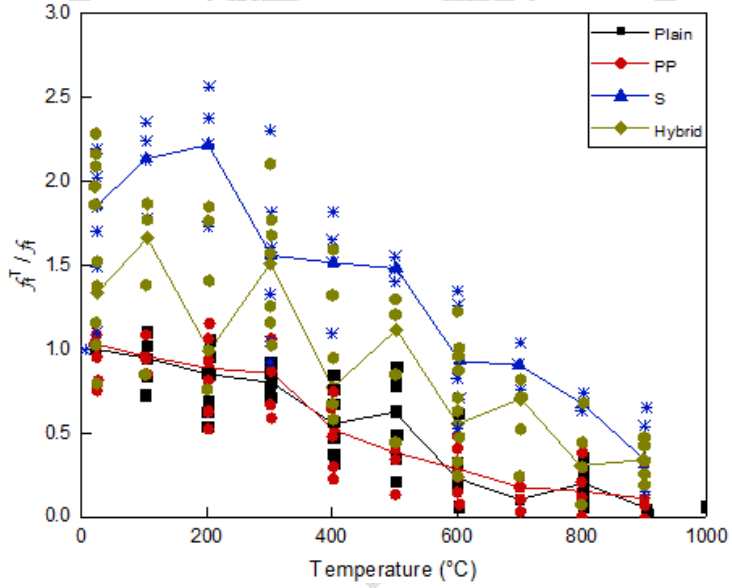

Fig. 12. Unstressed residual flexural strength of HPC

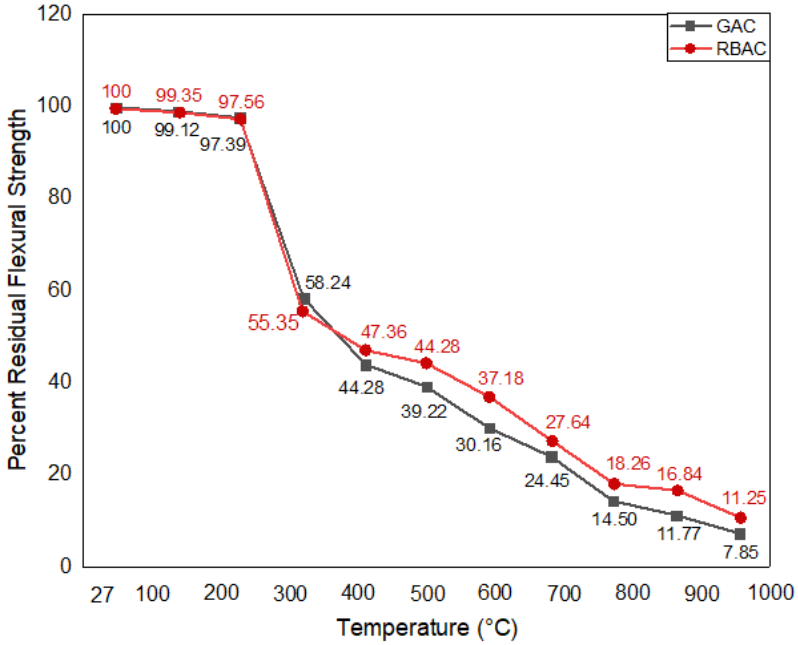

Fig. 13. Variation of residual flexural strength of GA and RBA concretes.

2.6. Shear strength

This study investigated the results of 15 papers, The shear strength was presented the various parameters on the residual of mechanical properties of concrete after exposures to elevated temperatures. Such as design of shear reinforcement and reinforced concrete rectangular beams using the latest edition of the Building Code Requirements for structural concrete. Shear strength for concrete beams and the lower and upper bound of shear strength requirement, shear force at the section, the difference between the cracking shear stress and ultimate shear stress, different types of

aggregate and greed of concrete, failure and cracking of concrete. Jose that the shear strength of the beam is considered to be the sum of shear strength provided by the concrete and that attributable to the shear reinforcement the nominal shear strength provided by the concrete calculated as:

$$V_c = 2\sqrt{f'}\ b_w d \qquad (13)$$

The value of $\sqrt{f'}$ in the equation 14 is limited to a maximum of 100 psi. The shear reinforcement may consist of stirrups perpendicular to the axis of the member, welded wire fabric with wires perpendicular to axis of member, spirals, circular ties, or hoops.

$$\phi V_n \geq V_u \qquad (14)$$

Where, V_u is the factored shear force at the section considered and V_n is the nominal shear strength computed as :

$$V_n = V_c + V_s \qquad (15)$$

V_s can be expressed as:

$$V_s = V_n - V_c = \left(\frac{V_u}{\phi}\right) - V_c \qquad (16)$$

Where, V_c is the strength provided the effect concrete section and V_s is the strength provided by the shear reinforcement. The strength reduction factor ϕ is 0.75 (ACI 318 section 9.3), a change from previous code revisions of 0.85. In computing V_c, the effect of axial tension or compression will not be considered for this course (Jose-Miguel Albaine, 2012).recommended that the shear strength decreased with the increase of high-impact polystyrene (HIPS) aggregate. The percentage decrease in shear strength at 50% replacement at 7-day and 28-day was 58.14% and 52.63%, respectively. The percentage retention of shear strength at 50% replacement at 7 d and 28 d was 41.86% and 47.37%, respectively (Senthil Kumar, 2014). It was found that the more significant shear strength increases with fiber-reinforced high-strength concrete specimens (60% with

steel and 17% with polypropylene fibers) than with fiber-reinforced normal strength concrete specimens (Uttam B. Kalwane, 2016).

$$\tau_s = \frac{P_{max}}{2b_{eff} \times d_{eff}} \qquad (17)$$

Where,

τ_s =ultimate shear strength in N/mm²

P_{max} =the average peak load supported by the concrete prism in kN

b_{eff} =the effective width of the specimen in mmm

d_{eff} =the effective depth of the specimen in mm.

It can be noted that the concrete shear strengths for concrete mixes with aggregate replacement were not significantly different from those of standard concrete of comparable shear strength. Therefore, a regression equation was developed to estimate the shear strength of concrete with a coarse aggregate replacement, not beyond these levels of replacement (Folagbade Olusoga Peter ORIOLA, 2017). It was reported that the self-compacting concrete (SCC) plain self-compacting concrete (P-SCC) and end-block strengthened self-compacting concrete (R-SCC) were used to study the inclined shear plane on the shear strength. In the case of R-SCC, shear strength was approximately the same at 22° and 31°. In the case of plain SCC, there was not much difference between the cracking shear stress and ultimate shear stress indicating sudden failure (Harish Kumar N R, 2015). studied that the shear strength (using push-off specimen) of SCC and normal cement concrete (NCC) of grade M30 (representative of standard strength concrete) and M60 (representative of high strength concrete). Shear strength tests (using push-off specimens) were has conducted at 14 days and 28 days of curing change in shear strength with an increase in the grade of SCC (Mr. Prasad V, 2019). It was noted that the experiment results showed that the shearing strength depended considerably on the percentage of replacement of natural coarse aggregates (NCA) with recycled aggregate concrete (RCA). The results of an experimental study of the push-off shearing strength of normal-strength plain (RAC). It can negatively affect the properties of the produced concrete, especially those who rely significantly on the properties of the aggregates (Rahal., 2017). The experimental results showed that the shear strength of reinforced concrete walls with boundary members, as reported in the previous literature, is larger than the shear strength of reinforced concrete walls without boundary members. The walls with boundary member effect indicated a shear strength higher than that without boundary member effect (Ika Bali, 2016). The shear strength of concrete is an ability to resist forces that cause sliding of one-part relative to the other internal plane. The reported studies indicate that an increase in a volume percentage of steel fibers reasons increase the shear strength for both the grades of concrete. The shear strength of concrete increases as the percentage of fibers has increased. The increase in shear strength of both M30 and M60 grades of concrete as fiber percentage increases is substantial. The shear strength of concrete increases with an increase in the percentage of fibers (Mr. Chandrashekharamurthy H. K, 2019).

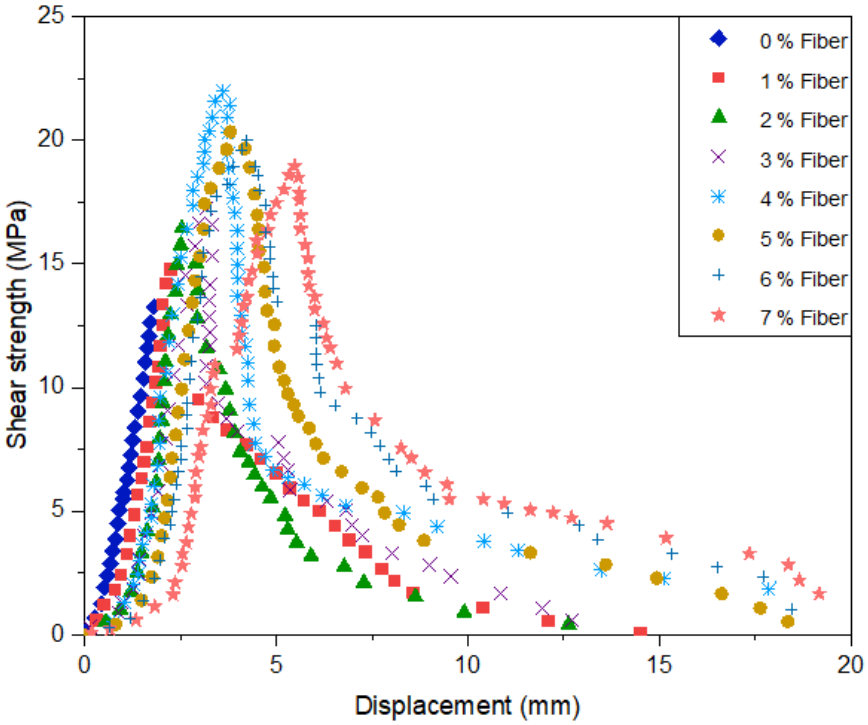

Fig.14. variation of shear strength (τ_{max}) with respect to displacement (γ) (double shear).

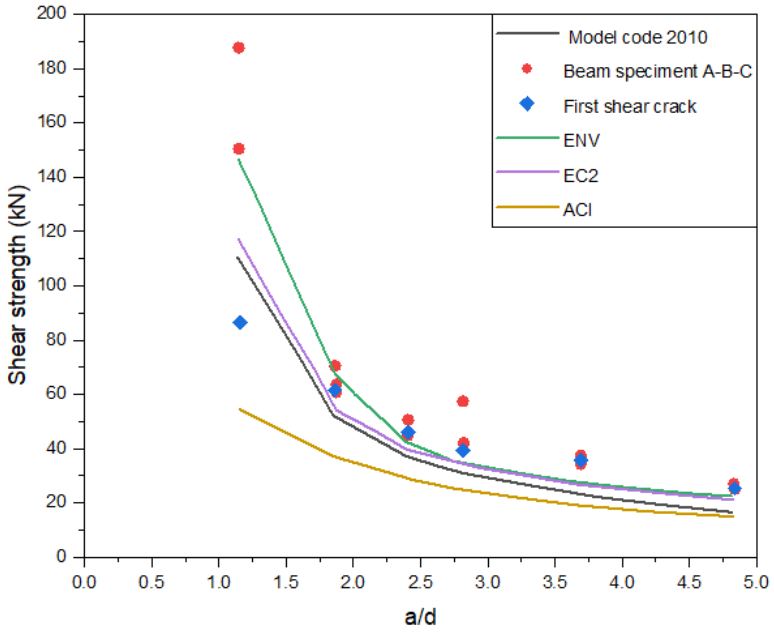

Figure .15. Shear strength of concrete at resistance load with beam specimen failure loads and load at the formation of shear crack data update from (ACI 318-08., 2007; CEN., 2004; Burssles:, 2004; Brussels, 1991; Bulletin, 2010; Nawy, 2009).

2.7. Elastic modulus

The elastic modulus (EM) of concrete is influenced by some factors which effected its compressive strength and tensile strength. The EM of concrete has been studied experimentally by various researchers. The EM of concrete including the composition of the concrete mixture, physical parameters of the components, the method of concreting, quality and quantity of the elastic, linear genetic programming (LGP) technique, different aggregates, and micro-contact printing. investigated the EM for each specimen was calculated from the modulus-porosity linear regression achieved for all 74 specimens by using the regression to extrapolate modulus values to zero vascular porosity. Numerous notably, due to the cumulative effects of small differences in EM between the two types of bone tissue, tissue strength for a given EM is higher by 20–30% for cortical bone (Bayraktar, 2004). studied that the modulus of elasticity of both NSC and HSC seems to be in direct proportion to the cube root of compressive strength, according to the European Code10-11 rules. Theoretical and experimental approaches can be applied to evaluate the EM of concretes. The theoretical model, concretes are assumed to be a multi-phase system; thus, the modulus of elasticity achieved as a function of the elastic behavior of its components. Theoretical models can appear too complicated for a practical purpose because the EM of concrete is a function of several parameters as a consequence, such models can only be used to evaluate the effects produced by the concrete components on the modulus of elasticity (Noguchi, 2009). reported that the LGP-based models relate the modulus of elasticity of NSC and HSC to the compressive strength, as similarly presented in several codes of practice. The models are developed based on experimental results collected from the literature. The LGP technique is utilized to find mathematical relationships between the elastic modulus and the compressive strength of NSC and HSC (Gandomi, 2010). studied the modulus of elasticity (E) of difference concretes at chamber temperature vary over a wide limited, 5.0 × 103 to 35.0 × 103 MPa, and is relevant mostly on the water-cement ratio in the mixture, the era of concrete, the technique of limited, and the quantity and nature of the aggregates. The modulus of elasticity losses rapidly with the ascent of temperature and the aliquot reduction does not depend significantly on the aggregate (C. R. Cruz).proposed that the static EM of concrete were calculated with the Eq. (18) The residual EM of concrete was different at 7 and 28 days up to 600°C.

$$E = \frac{S2\_S1}{\varepsilon 2\_0.000050} \qquad (18)$$

Where, S_2 is the stress corresponding to 40 % of ultimate load; S_1 is the stress corresponding to a longitudinal strain of 50 millionths; and ε_2 is the longitudinal strain caused by stress S_2. The values of S_1, S_2, and ε_2 were determined from the stress-strain curve both at ambient and elevated temperatures (Lodi., 2017).The purpose of this study was to measure the modulus of elasticity of dry, mature maize rind tissues using three different loading modes (bending, compression, and tensile), and to determine the accuracy and reliability of each test method. The three testing modes produced comparable EM values. For the sample in this study, modulus values ranged between 6 and 16 GPa. It was indicating spatial variation in the modulus of elasticity between the nodal and internodal regions (Al-Zube, 2018). detected the presence of the equation provides the most accurate prediction for the EM of FRC and FRCC with a coefficient of variation of 15% as compared to 32% using ACI 318 equation for coarse aggregate weight/sand aggregate weight (C/S≥1). The elastic modulus of the cylinders under compression was measured using a linear variable displacement transducer (LVDT) at the midweight of the cylinder. To further examine the impact of discrete fibers on elastic modulus, a comprehensive elastic modulus database had been gathered using experimental results obtained from various works of literature listed. All equations that depend on the elastic modulus of standard concrete also have a high coefficient of variation of elastic modulus data (COV) when using ACI 318 to predict the elastic modulus of standard concrete with COV exceeding. As a result, existing elastic modulus equations from the codes would not provide a reasonable estimation of the reduction in elastic modulus (Suksawang, 2018).recommended the relationship between compressive strength (CS) and age and between the modulus of elasticity and CS had analyzed. The average 28-day EM of concrete, obtained from three specimens in each case, ranges between 22 and 40 GPa, with a standard deviation ranging between 0.05 and 2.2 GPa, as shown in Table 3. As expected, the EM of concrete increases with its CS comparison of the measured mean elastic (T. Sakthivel, 2019).

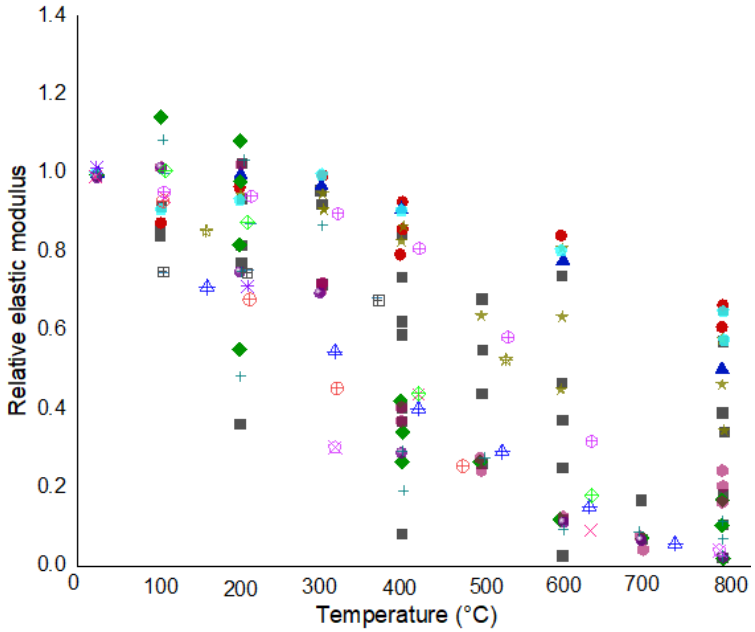

Fig.16. Residual modulus of elasticity of concrete at elevated temperatures.

3.1. Yield strength

The yield strength (YS) is more critical on the residual properties of steel reinforcement were presented both of the YS in tension and compression. Mostly focused on the yield of compressions. However, it is essentially vital when steel reinforcement subjected to elevated temperatures. Moreover, the YS has been suggested to various parameters on the residual of steel reinforcement at the elevated temperatures. The details of the YS teste result from different articles. Were some parameters proposed, such as calculation design of steel structures elements, different in tension and compression, Different valve of the steel bars, and steel-reinforced concrete-filled steel tubular (SRCFST) columns under axial compression of YS, friction stress, grain size hardening, and well-constructed solution hardened with carbon and differences in the YS for structural steel proposed by different codes. Furthermore, the YS details are essential for the calculation and design of steel structures elements. Interestingly, the outline starts to change, and the YS zone almost disappears. Reuse hides its risks and should be approached by experimentally proving the strength properties of the corroded material (Shopov, 2019). recommended that the material properties of the tests for high strength steel and mild steel at average room temperature. Also, they determined from the ratio of different YS at different temperatures (22°C) for the strain levels of 0.2,0.5,1.5and 2.0%. Ignasi et al. [114] a common concept that the yield stresses measured in the monotonic tests were found strongly dependent on the corrosion degree. Corrosion of steel highly reduces the yielding stresses (Chen, 2006). it was found that the use of the 0.2% offset method to define the YS of gradually yielding reinforcing steel is safe and realistic (Ignasi Fernandez, 2015). According to the ACI code depth-span limitations tabulated for standard weight concrete and specified YS of steel, for other values of steel yield strength and lightweight concrete, correction factors are provided (Paulson, 2016). study revealed that going by the common suggestion by the professionals to reduce the YS of steel bars to 410N/mm2, about 28% and 33% of 12mm and 16mm bars, respectively, failed to meet the 410N/mm2 criterion (Anthony Nkem Ede, 2014). Reported that the YS and isotropic hardening behavior might be different in tension and compression. Different yield criteria and plastic flow potentials used for tension and compression. The used model material has YS and isotropic hardening behavior and was different in tension and compression (Gadea, 2019). The available literature of the YS ratio are higher than the values set by BS 4449 and SSMO 1577 (Taghried Isam Mohammed Abdel-Magid., 2017). investigated that the ductile high strength steel, which has a YS ranging from 520 to 1000 MPa, is commercially available due to advances in nontechnology. However, The ACI-318-08 building code requirements for structural concrete specifies that the YS must be taken as the stress corresponding to a strain of 0.35% when high strength rebars. [f_y more than 410 MPa]. This condition limits the YS to be less than 680MPa. Also, a recent study concluded that for serviceability and cracking control, stresses in steel should be limited to 50% of the YS to have a similar performance of Grade 60 steel. An increase of YS decreases the ductility because it increases the yield strain (f_y/E_s); therefore, φ_u/φ_y it is decreased ((Sherif

Yehia., 2011). studied the YS of polycrystalline Nanotwinned copper (Nt-Cu), can be evaluated based on the Sachs model (Barnett, 2006). Results show that the calculated YS increased, and the λ decreased from 100 nm to 15 nm, where the YS Nanotwinned polycrystalline copper (Nt-Cu) YS to get the maximum value of 940 MPa. When λ goes below 15 nm, the strength decreases with a smaller λ (Xiao J. e., 2019). illustrate the assumed material curves, with four changing parameters α (length of the plastic plateau), β (reinforcement index), and γ (initial rigidity of reinforcement) as well as YS fy = 200, 400, 600, 800 and 1000 MPa. Young's modulus equaled E = 200000 MPa. (Korentz, 2010). noted that the variability of YS of reinforcing steel bars play an essential issue in the reliability study of such structures and the development of strength-reduction factors. YS of reinforcing steel bars constitute the most necessary primary data while analyzing the reliability of such bars (Lubna S. Ben Taher, 2013). suggests a coefficient of variation of 5% for each of the two types of the above mentioned variations. Hence, the total variation in yield strength can be calculated as:

$$\delta_{total}^2 = \delta_{actual}^2 + \delta_{in\ sp.}^2 yeild\ strength \quad (19)$$

$$\delta_{total}^2 = (0.15)^2 + (0.05)^2 + (0.05)^2 \quad (20)$$

$$\therefore \delta_{total} = 0.165 \quad (21)$$

The value of $\delta_{total} = 16.5\ \%$ can be taken into consideration in studied the effect of variation of steel strength in the probabilistic study of the strength of reinforced concrete members (Mirza, 1979).

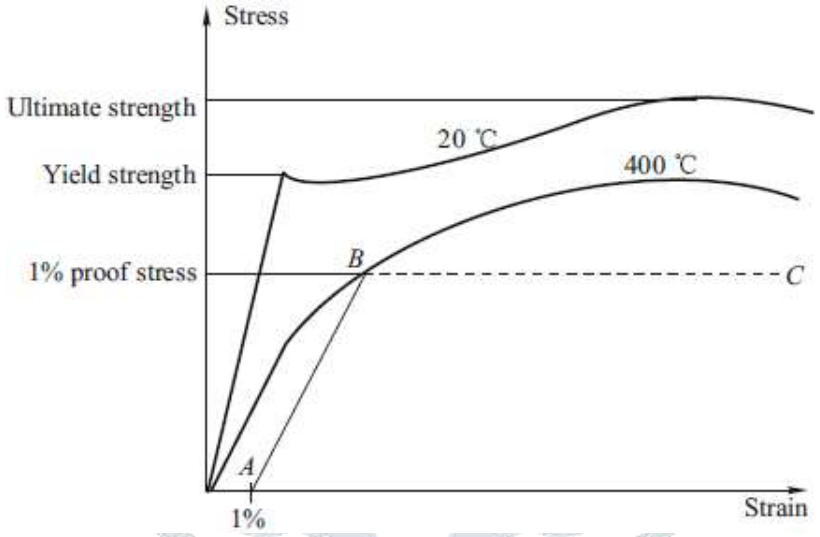

Fig.17. Definition of yield stress from (3:, 2005; 4:, 2005; T. R. Kay, 1996).

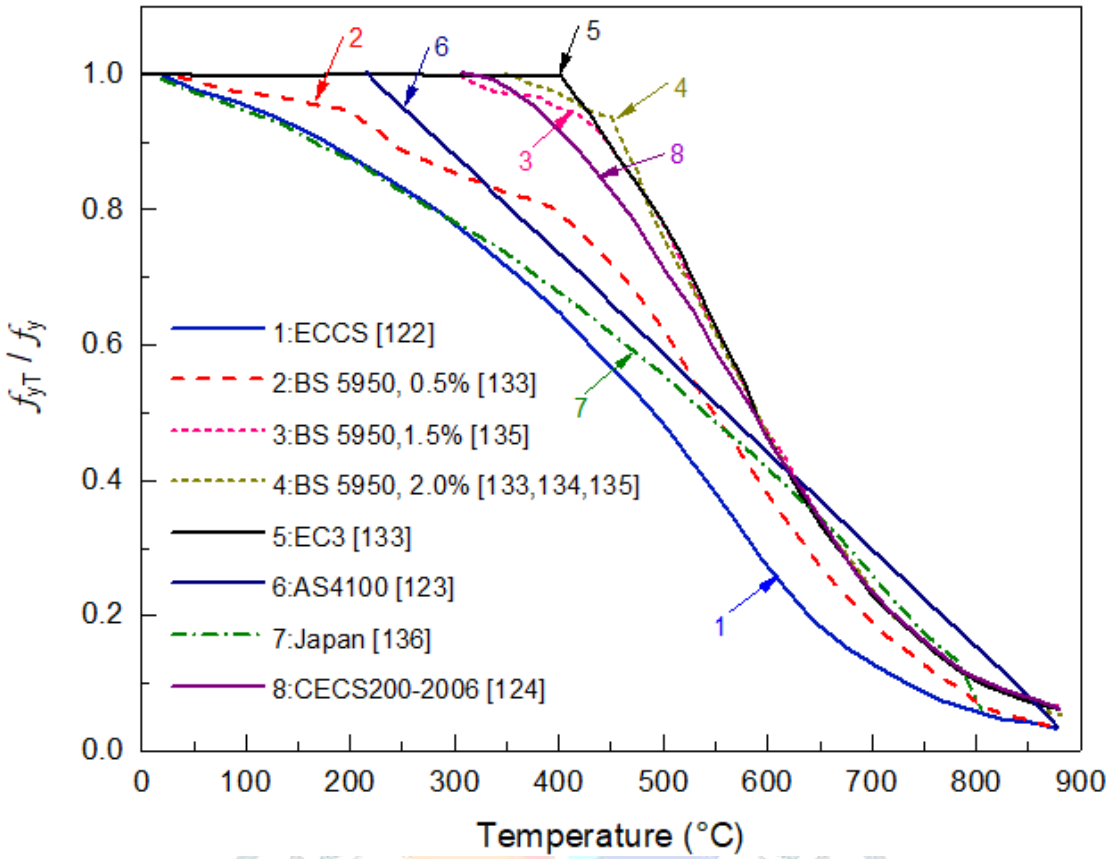

Fig.18. Yield strength of structural steel at elevated temperatures.

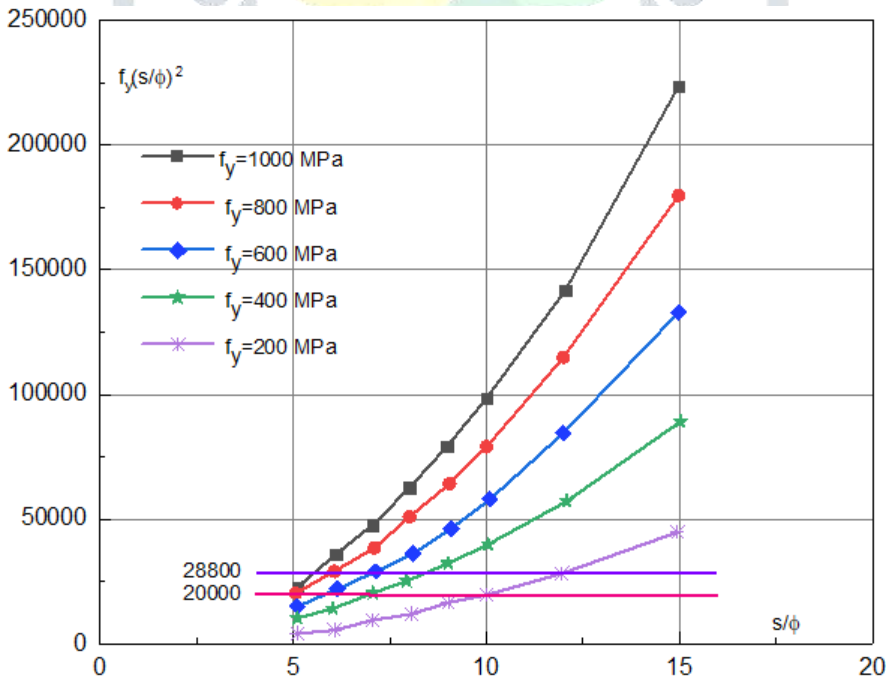

Fig.19. Graphs of relations $f_y(s/\emptyset)^2$ for various yield strengths [update from (Korentz, J., 2010)].

The static equilibrium paths for compressed bars with slenderness $s/\phi \leq 5$ overlap The material curve only for steel of yield strength $f_y = 400\ MPa$. The behavior of compressed bars in the state of post-critical deformation made of steel of the same strength characteristic depends on a single parameter described with expression $f_y(s/\phi)^2$.

3.2. Ultimate strength

Several studies have carried out on the ultimate strength of residual properties of steel reinforcement after exposure to elevated temperatures. Where well-thought-out such as elevated temperatures, ultimate limit, structural limits and safety margins, characteristic value of strength, uncertainties in the structural geometry, scantlings and imperfections, initial deflection shape and boundary conditions, energy dissipation capacity member, ultimate behavior of individual structural members, maximum value of the axial force and the type of steel structure models under axial compression undertaken and steel cracked plat. Czujko studied the ultimate strength (US) of loading exceeds structural capacity, and the structure collapses. For steel structures, aspects often checked in the ultimate limit state are resistance and stability. The US analysis leads to a more significant understanding of the structural performance and realistic expectations of structural limits and safety margins. They have affected the different material models applied when assessing the US, including the statistical variation of material properties and US assessment requirements, include checked the structural strength under the worst, extreme quasi-static loading conditions.

$$G = C_d - \sum D_{di} \geq 0 \qquad (22)$$

Where, G is the performance function C_d and D_{di} are the design values of capacity (strength) and i-th load component, respectively. (Czujko, 2018). investigated the effect of corrosion degradation on the US of the box girder is analyzed, and dissipated energy, compliance, ductility, and elastic limit are tested and discussed. A reduction in the elastic limit and the US of corroded stressed wire observed (Saad-Eldeen, 2012). The results indicate that the US behavior of a plate is significantly affected by parameters such as the initial deflection shape and boundary conditions of the plate, as well as loading conditions (J. K. Paik, 2009). noted that the residual stresses for encased steel profile might be included in the analysis, as described in the standard fire curve is used in this article to obtain the gas temperature. Where are presented the gas temperature (°C) and t is the time of exposure to fire in minutes. The US for each model without fire exposure was also calculated to provide an appropriate reference strength (Chiorean C.G., 2019). It has found that the double-hull tankers, a 10% loss of bottom results in a 4.4% loss in section modulus to the bottom, a 4% loss in section modulus to the deck, a 2.7% loss of US under hogging requirements and a 2.2% loss in the US under sagging conditions (A. W. Hussein. (2009). , 2009). It should be noted that the US often of more limited significance compared to the energy dissipation capacity member, determined on under the resistance – deformation curve for the member. Also, explained the increase of acceptance and use of structural reliability techniques requires the US discussion to include the possible use of strength prediction tools and information in a structural reliability-based process. The ultimate behavior of individual structural members can be considered as the first useful step to understand the overall structural performance and to predict potential failure mechanisms of more complex structures (Dr. M.L. Kaminski., 2000). recommended that the maximum value of the axial force is the US. It can for more extensive research regarding the US instead of using costly nonlinear FEM. The beam-column US calculated by this method can be used effectively to predict stiffened panel US using the beam and column model (Zhongwei Li, 2017). The addition of US interaction relation for a perfect plate between biaxial compressive loads.

$$\left(\frac{\sigma_{xav}}{\sigma_{xu}}\right)^2 + \left(\frac{\sigma_{yav}}{\sigma_{yu}}\right)^2 = 1 \qquad (23)$$

Where, σ_{xu} is the ultimate strength of a plate under longitudinal axial compression alone, and σ_{yu} is the ultimate strength of a plate under transverse axial compression alone. confirmed that Eq. (50) (Kee Paik, 2008) US decreases characteristics of plate elements due to cracking loss are considered with varying size and location of the cracking loss, both experimentally and numerically. The US tested the type of steel structure models under axial compression undertaken. Table 5 summarizes the US of cracked plates with varying crack size and location, obtained from the present experiments. Therefore, the ultimate strength of the steel cracked plate subjected to axial compressive loads can then be predicted using Eq. (24)

$$\sigma_{xu} = \frac{A_c}{A_o} \qquad (24)$$

Where, σ_{xuo}, σ_{xu} are the ultimate axial compressive strengths of uncracked (intact) or cracked plating, A_o is the total cross-sectional area of untracked (Paik, 2005) investigated the effect of pitting corrosion on the US of plates subjected to in-plane compression and bending, a series of nonlinear FE analyses have reported with plates having a variety of pit distributions. The reduction in the US due to pitting corrosion is almost independent of the stress gradient (Nakai, 2006). Paik et al. [150] study the residual US characteristics of steel plates with cracking damages under axial compressive actions through experimental investigations (Jeom KeePaik., 2008). According to the influence of excellent location and crack length on the US characteristic soft hose structural elements under monotonic longitudinal axial compression. In order to examine the effect of crack length on the US characteristics, the crack location has been constant while its length alters (Bayatfar, 2014). The main objective of the present paper is to numerically examine the residual US characteristics of steel plates with longitudinal cracks under axial compressive actions. Only a small change of the US appears due to the size of crack — residual stresses, which may further reduce the ultimate plate strength in reality (Paik J. K., 2009).

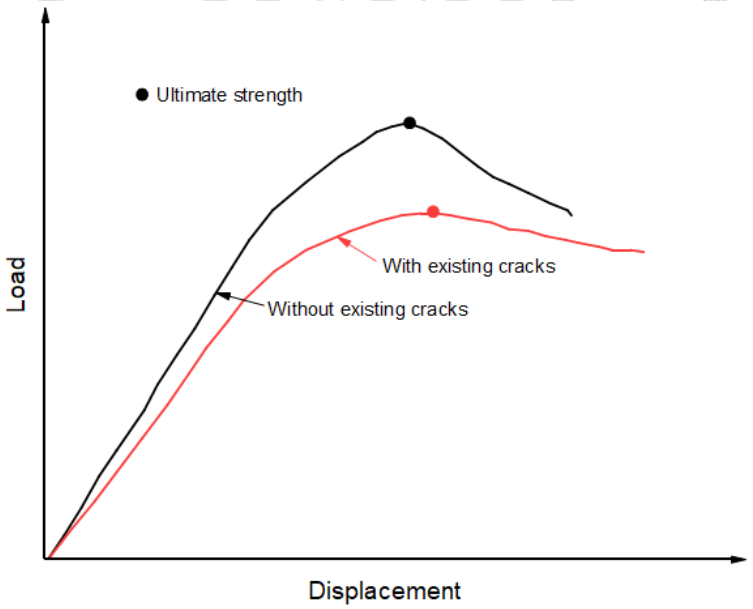

Fig.20. A schematic representation of the cracking damage effect on the ultimate strength behavior of steel structures.

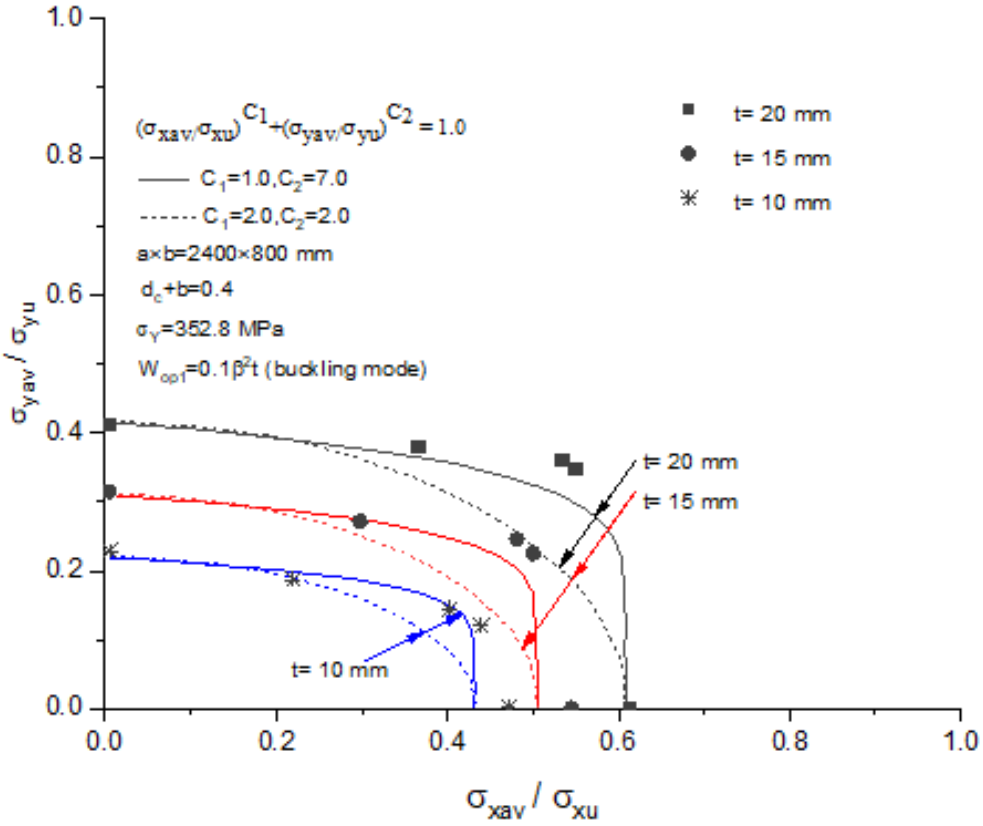

Fig.21. ultimate strength interaction relationship of a perforated steel plate under biaxial compression with varying the plate thickness.

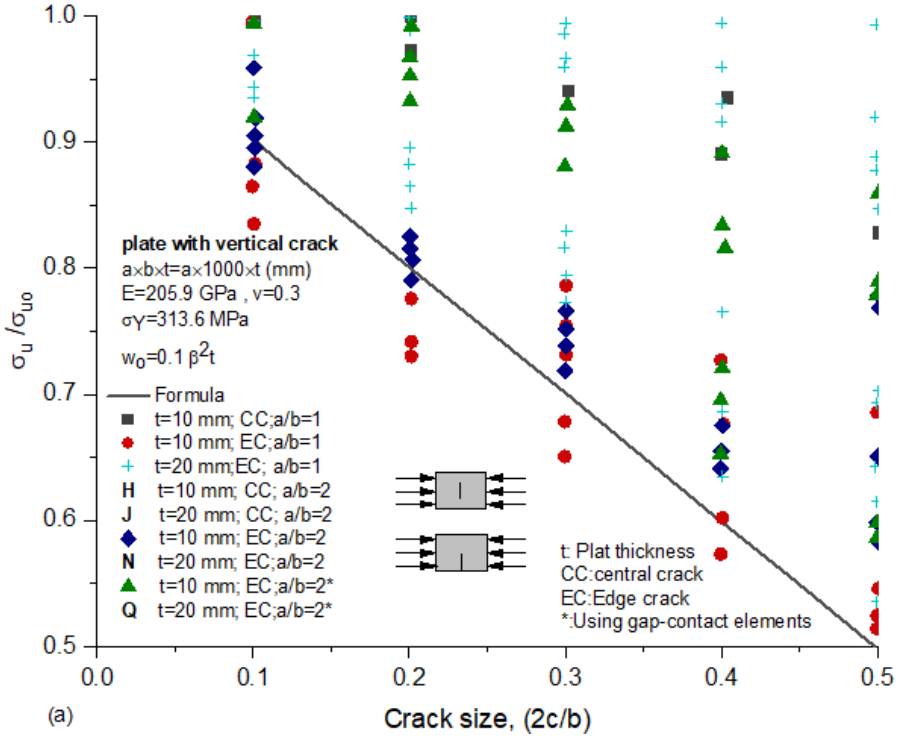

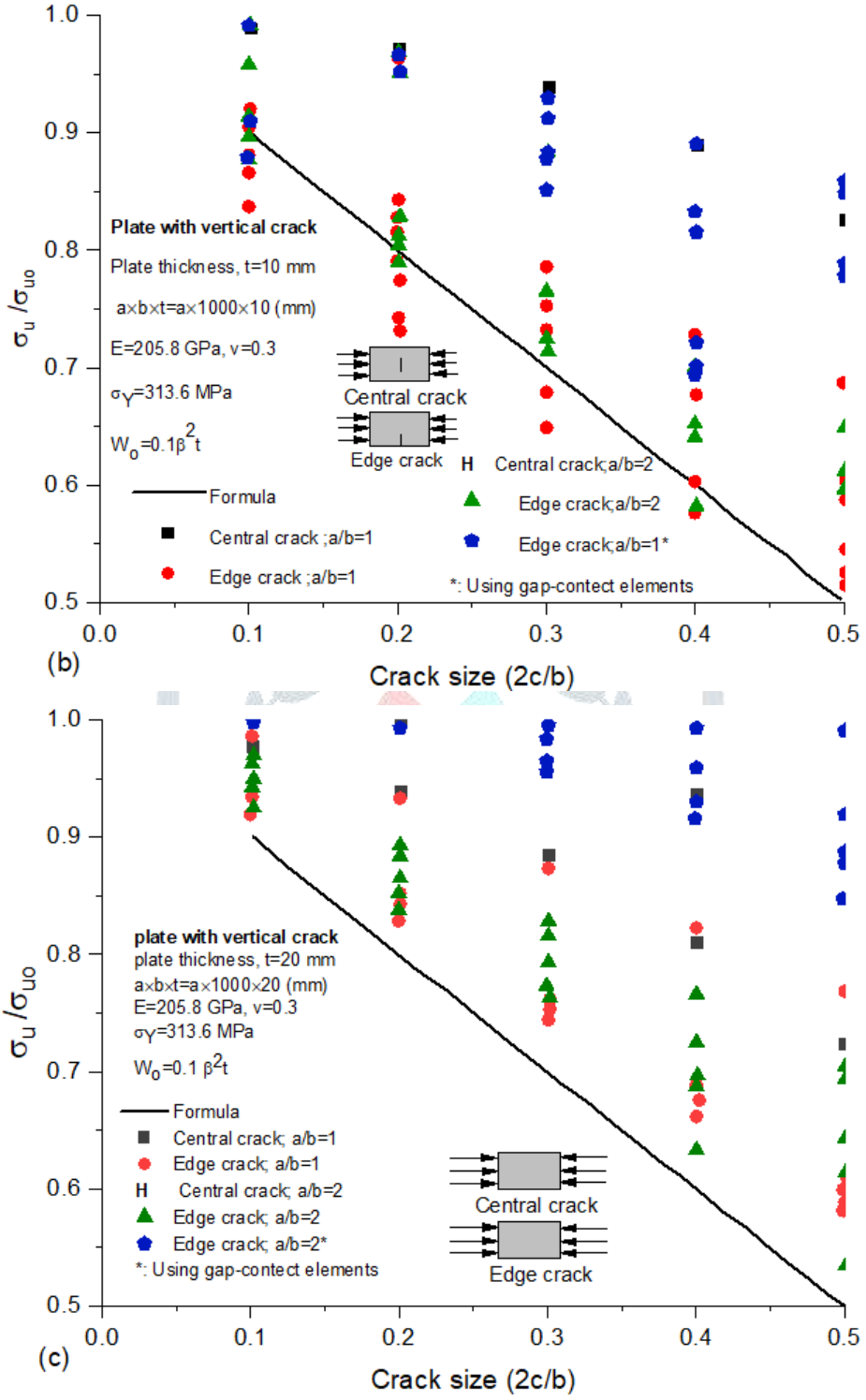

Fig. 22. (a) The ultimate compressive strength reduction characteristics of a cracked plate as a function of the crack size with varying the plate thickness and the plate aspect ratio. (b) The ultimate compressive strength reduction characteristics of a cracked plate as a function of the crack size, t=10 mm. (c) The ultimate compressive strength reduction characteristics of a cracked plate as a function of the crack size, t= 20 mm. (data adapted from (Paik, J. K., Kumar, Y. V. S., & Lee, J. M., 2005)

.

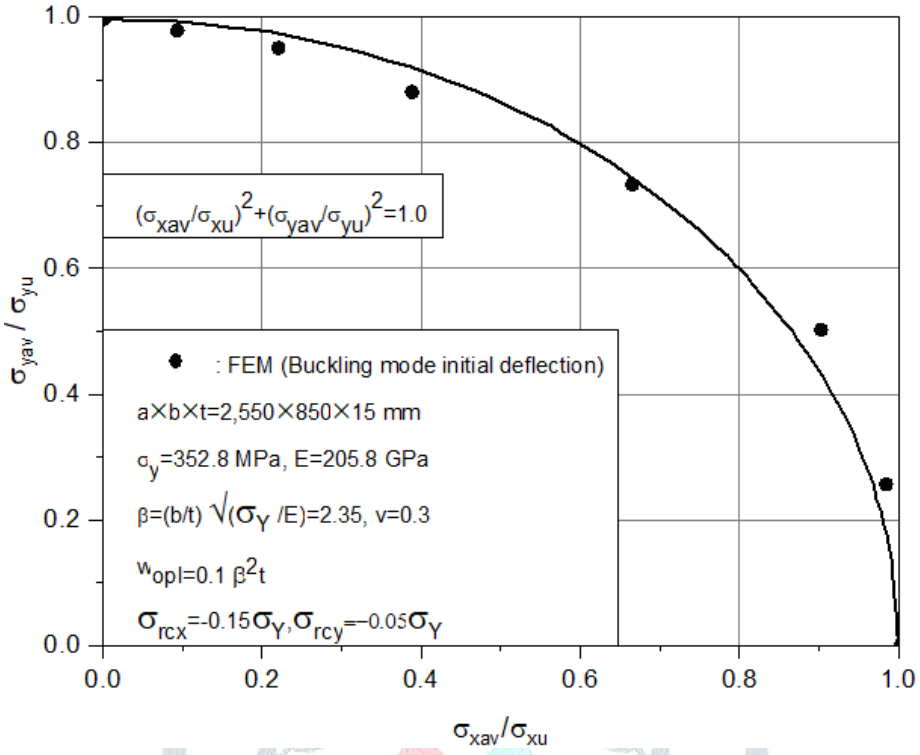

Fig.23. Ultimate strength interaction relationship of a perfect steel plate between biaxial compressive loads.

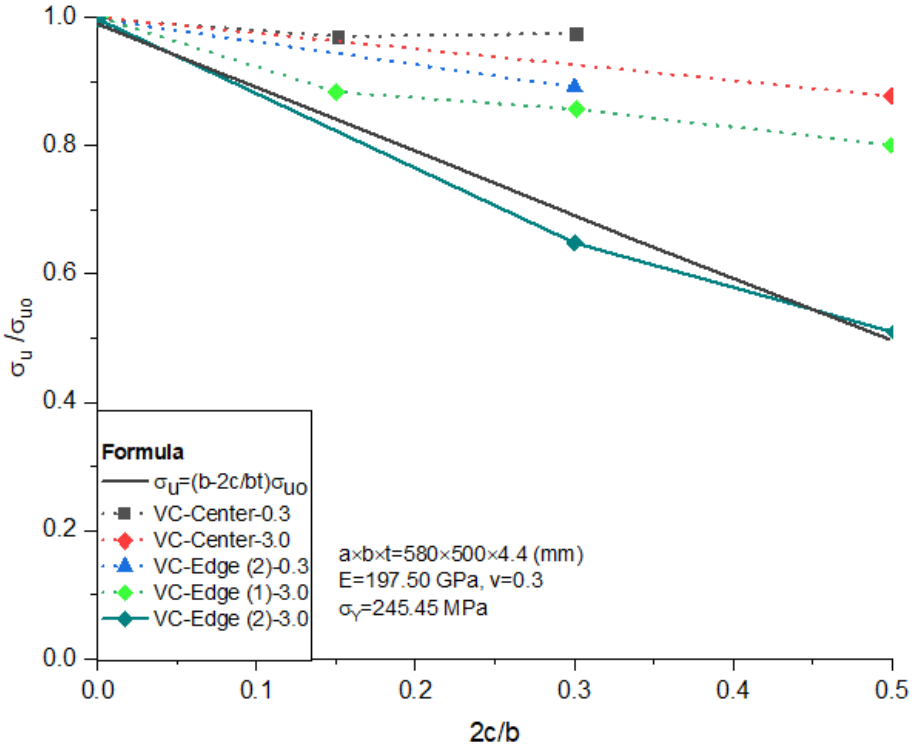

Fig.24. The ultimate compressive strength reduction characteristic of steel plates as a function of the crack size (σ_{uo}, σ_u, ultimate strength of uncracked or cracked plate elements).

3.3. Elastic modulus

Elastic modulus (EM) is a material property that shows the strength or elasticity of the steel materials used for making mold parts. The EM generally It had influenced by some factors which more utilization. Various researchers have studied the EM of residual properties of steel reinforcement. Such as grade of steel and thickness, high-temperature diffusion self-lubricating material decreases, reasonable agreement, EM increased until the steel fiber index is 50, Comit Euro-International du B ton (CEB) and the F d ration International de la Pr Contrainte (FIP), a numerical model to the effects of aggregate and fiber random distribution on the EM of steel fiber reinforced concrete (SFRC). Aggregate and fibers, EM equations static EM at room temperature, EM Resonance Frequency (EMRF) values, resonance frequency (RF), and ultrasonic pulse velocity (UPV), The dynamic EM from UPV values calculated equations, the EM of Hybrid Fibers Reinforced Concrete (HFRC). Using two indices, one is the coefficient of variance (COV), and the second is the coefficient of determination. investigated the modulus of elasticity, and the current method is to assume it to be about 200 GPa for all steel grades. However, compressive tests of these steels have consistently noted that the modulus of elasticity varies with grade of steel and thickness (Mahendran, 1996). The author notes that composite EM of the high-temperature diffusion self-lubricating material decreases with temperature and velocity and increases, including the load (Xie, 2018). noted that the increase of strain at peak stress additionally presented a good agreement with the increase of fiber amount fraction. It has further concluded that the modulus of elasticity increased with an increase in fiber volume fraction or fiber reinforcing index (Gul, 2014). studied that the elastic modulus assumption formula is as follow:

$$E_c = \gamma^{1.5} 4270 \sqrt{f'_c} \qquad (25)$$

$$E_c = \left(\frac{\gamma}{2.346}\right)^{1.5} \left(10500 \sqrt{f'_c} + 70000\right), \qquad (26)$$

$$E_c = k_1 \sqrt[3]{f'_c}, \qquad (27)$$

$$E_c = k_1 k_2 \times 40250 \left(\frac{\gamma}{2.4}\right)^2 \sqrt[3]{f'_c}, \qquad (28)$$

$$E_c = \left(\frac{\gamma}{2.4}\right)^{1.5} \left(10000 \sqrt{f'_c} + 73000\right), \qquad (29)$$

Here, E_c, fc ′, and γ represent EM of concrete (kgf/cm²), compressive strength (kgf/cm²), and unit weight (t/m^3), respectively, and $k1$ is the coefficient of coarse stone aggregate type. For example, in the case of limestone aggregate, Comit Euro-International du B ton (CEB) and the F d ration International de la Pr contrainte (FIP). Model Code. proposes 0.9, and new RC Project proposes 1.2, while the value of $k2$ of 0.95-1.1 is a coefficient related to the use of admixture (Jang. I.Y., 1996). presented the offers a mesoscale numerical model to the effects of aggregate and fiber random distribution on the EM of steel fiber reinforced concrete (SFRC). Results show that the non-homogeneity of the matrix and irregular distribution of aggregate and fibers manage to disperse the calculated efficiency factor of fiber with a standard deviation of 2.5% to 3.0% (for 150 mm cube specimens, it can be different for other specimens (Shadafza, 2016).presented the equation provided the most reliable prediction of EM if the experimental EM of standard steel fiber with concrete is avail-able (Aslani, 2014). As a result, existing EM equations from the codes would not provide a reasonable calculation of the reduction in elastic modulus. Therefore, a new EM equation is proposed to better estimate the EM of FRC, including the most significant fiber volume fraction of 10% (Suksawang, N., Wtaife, S., & Alsabbagh, A., 2018).recommended that the relative values of EM as a function of temperature. The static EM at room temperature is 38.63 GPa. In contrast, the calculated dynamic EM from and ultrasonic pulse velocity (UPV) and RF values are 45.9 GPa and 38.03 GPa, individually. The dynamic EM Resonance Frequency (EMRF) values are more close to the static EM. The residual mechanical properties, resonance frequency (RF), and UPV considered as a function of temperature. The result shows that the residual strength increases from room temperature to 300°C. However, above 300°C, it is decreasing gradually. Various comparisons have made between residual mechanical strength versus UPV and RF measurements (Hou, 2017).showed that the calculation of dynamic EM. The dynamic elastic modulus from UPV values calculated from the following equation; (ASTM, 2016.)

$$E_d = \frac{\rho v^2 (1 - \upsilon)(1 - 2\upsilon)}{(1 - \upsilon)} \qquad (30)$$

Where.

E_d — is the dynamic EM,

υ — is the Poisson's ratio, Calculated,

ρ — is the residual density (Kg/m^3), measured from the residual weight. □

V — is the ultrasonic pulse velocity (km/s)

It was found that the EM parameter that is defines the elastic behavior of a material. Accordingly, there is a need to experimental investigate mechanical behavior such as the EM of Hybrid Fibers Reinforced Concrete (HFRC). Using two indices, one is the coefficient of variance (COV), and the second is the coefficient of determination (r^2) given by the Eq. 31 and Eq. 33, respectively

$$COV = \frac{\sqrt{\frac{1}{n-1}\sum_{i=1}^{n}(E_{cp} - E_e)}}{\mu} \quad (31)$$

Where, E_e and E_{cp} are the measured and predicted values of EM of HFRC, respectively and m is the mean calculated by the following equation:

$$\mu = \frac{\sum_{i=1}^{n} E_e}{n} \quad (32)$$

$$r^2 = \left(\frac{n(\sum xy) - (\sum x)(\sum y)}{[n\sum x^2 - (\sum x)^2][n\sum y^2 - (\sum y)^2]} \right)^2 \quad (33)$$

Where, x and y are the means of measured and predicted values of elastic moduli. The proposed equation for elastic modulus of HFRC with the maximum fiber volumetric-fraction of 1.9% based on the regression analysis ($r^2 \approx 65\%$) of 21 tested specimens was presented by Eq. (34 (Q.Z. Khan, 2019)

$$E_{cp} = 1508\sqrt{f_c'} + 6695(MPa) \quad (34)$$

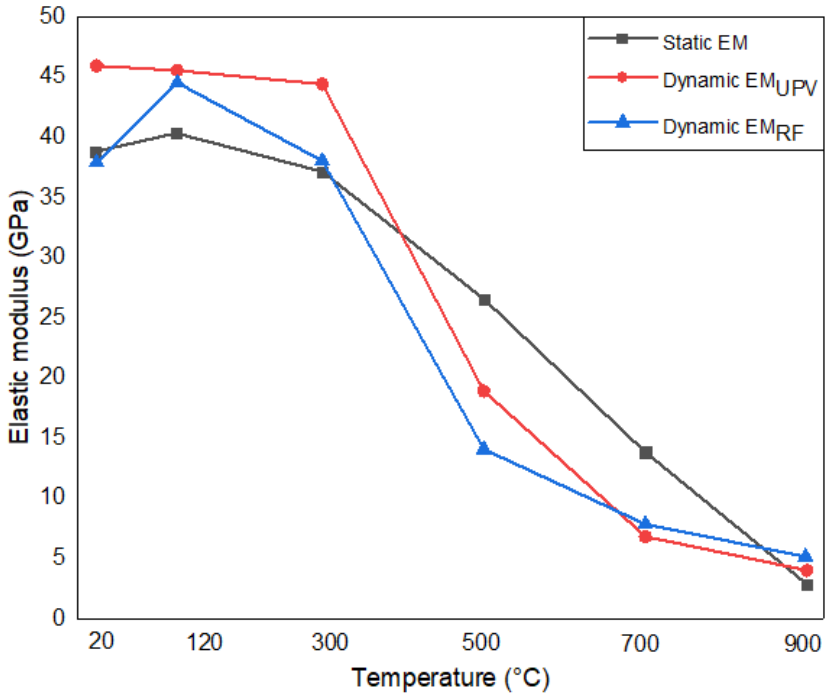

Fig.25. Elastic modulus as a function of temperature

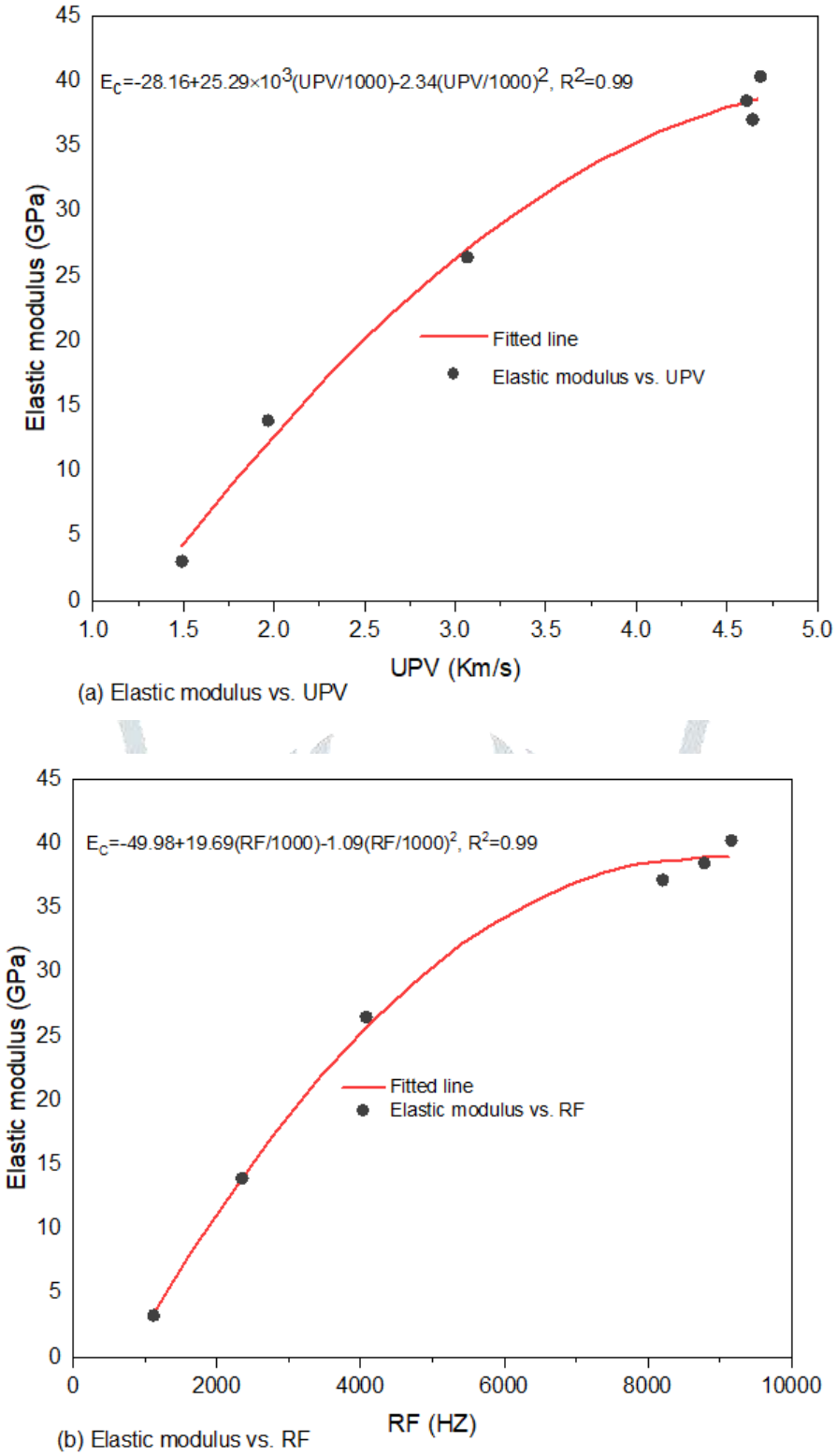

Fig.26. a and b relationship between mechanical properties vs nondestructive tests (NDTs).

3.4. Stress-strain curve

The residual properties of steel reinforcement most often expressed in the form of stress-strain relationships, which generally used as input data mathematical models for elevating the fire-resistant of the steel reinforcement members. Where well-thought-out Such as mathematical relationships reinforced steel at elevated temperatures, hot-rolled and cold-worked reinforcement, steel fiber reinforced all-lightweight- aggregate concrete (SFRLAC). The stress-strain of steel fiber reinforced and Circular steel tube confined reinforced concrete, the corresponding variations of G20Mn5QT, G20Mn5N and G20Mn5QT steel tested, hot-rolled steels High-grade Q420, fire exposed RC beams on maximum rebar temperatures consideration and very high strength steel S960 at ambient temperature. Investigated the analytical into the effects of stress-strain relationships (SSRs) on the fire show the steel beams and composite steel-concrete beams exposed to uniformly increasing temperatures on three sides (Buchanan, 2004).study has presented a new mathematical relationship for representing the SS behavior of reinforced steel at elevated temperatures. In the case of steel, the SSR is often assumed that to be elastic-perfectly plastic and expressed accordingly as

$$\sigma = \frac{\varepsilon}{2|\varepsilon|}\left\{ a - |a| + \left[\frac{(\beta_2-\beta_3)b}{\left(1+\left|\frac{(\beta_2-\beta_3)b}{\beta_5}\right|^{\beta_9}\right)^{\frac{1}{\beta_9}}} + \beta_3 b \right] \cdot \left[1 + \frac{|b|-|(b-0.001)|}{0.001}\right] \right\} \quad (35)$$

Where

$$a = \beta_1|\varepsilon| + \beta_4$$

$$b = |\varepsilon| - \beta_s - \frac{\beta_4}{\beta_1} \text{ and}$$

$$\beta_4 \frac{\beta_1}{E_{20}} = \frac{C_1 T + C_2}{(1+|C_3 T + C_{24}|^5)^{0.2}} + C_5 \quad (36)$$

$$\frac{\beta_2}{E_{20}} = \begin{cases} \dfrac{C_6 T + C_7}{(1+|C_8 T + C_9|)^{5^{0.2}}} + C_{10} T + C_{11} & \text{Where } T \le 500\ ^\circ\text{C} \\ \dfrac{\beta_1}{E_{20}} & \text{Where } T > 500\ ^\circ\text{C} \end{cases} \quad (37)$$

Where, E_{20} is the modulus of elasticity of steel; T is the temperature; β_i is the parameter controlling the shape of the stress-strain curve (SSC); ε is the strain; σ is the stress; C_i is the curve-fitting coefficient (Poh, 2001) noted that the simplified SS model had developed for reinforcing steel after exposure to elevated temperatures and cooling to room temperature. As standard hot-rolled reinforcing steel, no apparent influence of heat can be observed below 500 °C. The holding time of heating may affect the performance of prestressing steel after fire exposure during reinforcing steel (Tao, 2013).reported that the analytical model for SSC for steel fiber-reinforced concrete derived for concretes with strengths of 40 MPa and 60 MPa at the age of 28 days. The reinforced concrete with steel fibers with hooked ends 35 mm long and with an aspect ratio of 65 mm (Júnior, et al., 2010). presented the analytical model to get the complete SSC that was developed based on the model (CARREIRA, 1985).studied the evaluation of SS response and degradation of stiffness and strength properties and particular emphasis given to assessing the influence of temperature on enhancing the ductility of reinforcement. The expected variation in the shape of the SS response of hot-rolled and cold-worked reinforcement was evident in the steady-state tests (Elghazouli, 2009).it was found that the test conditions existed meant to simulate a building that had a fire, so the differences in the mechanical properties of reinforcing steels used in structures exposed to high temperature could be determined (Topçu, 2008.). The experimental results illustrated that the steel fiber volume fraction has a significant effect on the uniaxial compressive SSC of steel fiber reinforced lightweight concrete. Test results show that the peak-stress and peak strain at the SSC of steel fiber reinforced all-lightweight- aggregate concrete (SFRLAC) present an increasing trend with the increase of strength grade of cement and the volume fraction of steel fiber. Furthermore, the failure modes of specimens change from brittle failure to plastic failure with the increase of volume fraction of steel fiber (ZHAO Shunbo, 2019).investigated that the parameters included heat time, cross-sectional dimensions, the strength of the materials, steel tube to concrete area ratio, and the ratio of reinforcement. Finally, the design method suggested for divining the residual load-bearing capacity and compressive stiffness of circular steel tube confined reinforced concrete (CSTCRC) columns after standard fire exposure (Liu, 2014).investigated the mechanical properties of both casts of steel began to change after exposure to temperatures exceeding almost 700 °C. With increasing exposure temperatures, up to 1000 °C, G20Mn 5N showed that the maximum variations of approximately 28.6%, 14.8%, and 57% in yield strength, ultimate strength, and fracture strains, respectively; while the corresponding variations for G20Mn5QT were less severe at 16.8%, 7.6%, and 45%, respectively. The influence of different cooling methods was significant, notably when the exposure temperature exceeded 700–750 °C. The results of cyclic heating and cooling seemed insignificant. Predictive empirical equations to evaluate the post-

heating mechanical properties of the two cast plates of steel studied herein proposed for both air and water cooling (Lu, 2017) studied carried out the comprehensive knowledge of the post-fire mechanical properties of cast steels, assessing the residual performance of steel castings after fire exposure impossible. The experimental investigation into the post-heating mechanical properties of two widely used (in China) cast steels, namely: G20Mn5N and G20Mn5QT steel tested (K.J.N. Maclean, 2008).investigated hot-rolled Q235, Q345, and Q420 steels. Furthermore, the ultimate strength residual factors of all hot-rolled steels were related when they were cooled down from temperatures up to 700°C (Lu J. L., 2016). Kodur recommended that the approach is implemented using a detailed numerical model developed in the finite element. Predictions from the numerical model show a good relationship with the response parameters included in experiments for evaluating the residual capacity of fire exposed RC beams. Also, predictions of residual capacity from the finite element analysis compared with that collected from simplified

sectional analysis based on maximum rebar temperatures consideration. The comparison indicates that the finite element analysis yields more realistic predictions of residual capacity than that predicted from the simplified sectional analysis. The applicability of the given approach in evaluating the residual capacity of fire exposed RC beams shown through a case study (Kodur V. K., 2016).studied the residual SSR for reinforcing steel are determined using degradation trends reported (Neves I, 1996) noted that the post-fire SSC of stainless steel presented to different temperatures (200–1000 °C) and heat soak times (0–135min) were measured. The influence of different parameters on the elastic modulus, yield strength, ultimate strength, and ultimate strain. Based on the test results, the SS model proposed for austenitic stainless steel after exposure to fire (Wang, 2014).found that the comparison with design standards exposes the requirement of including stated theory on the deterioration of mechanical properties in the fire for very high strength structural steels in current leading design standards. The mechanical properties of very high strength steel S960 at ambient temperature and in the fire get from the SSC (Qiang, 2016)

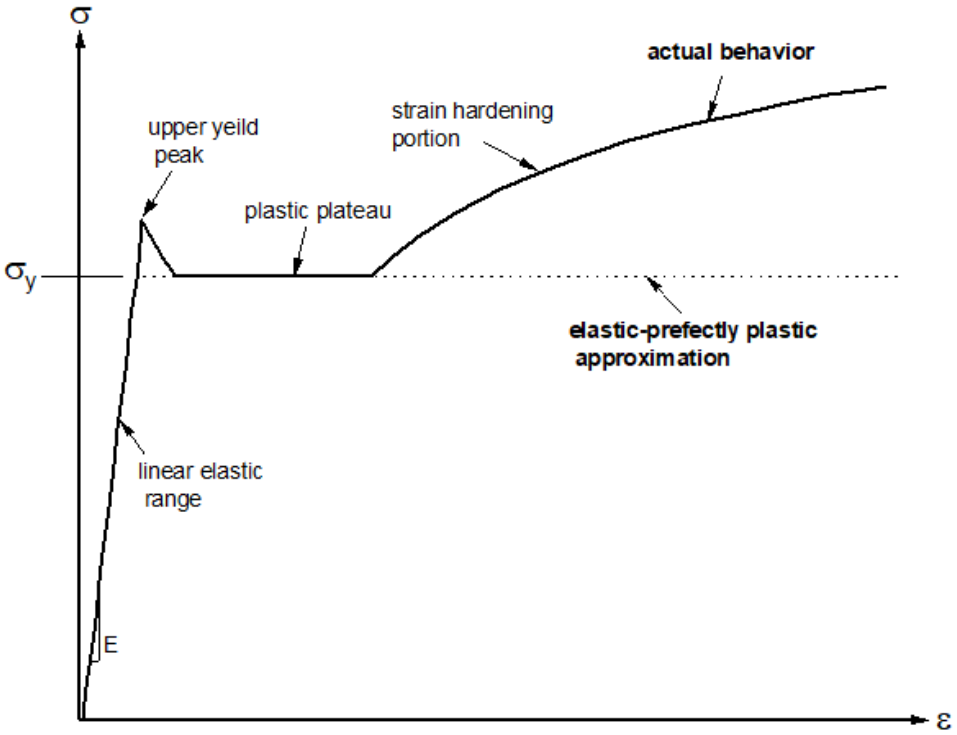

Fig.27. Stress-Strain Curve of steel and Elastic-Perfectly Plastic Approximation.

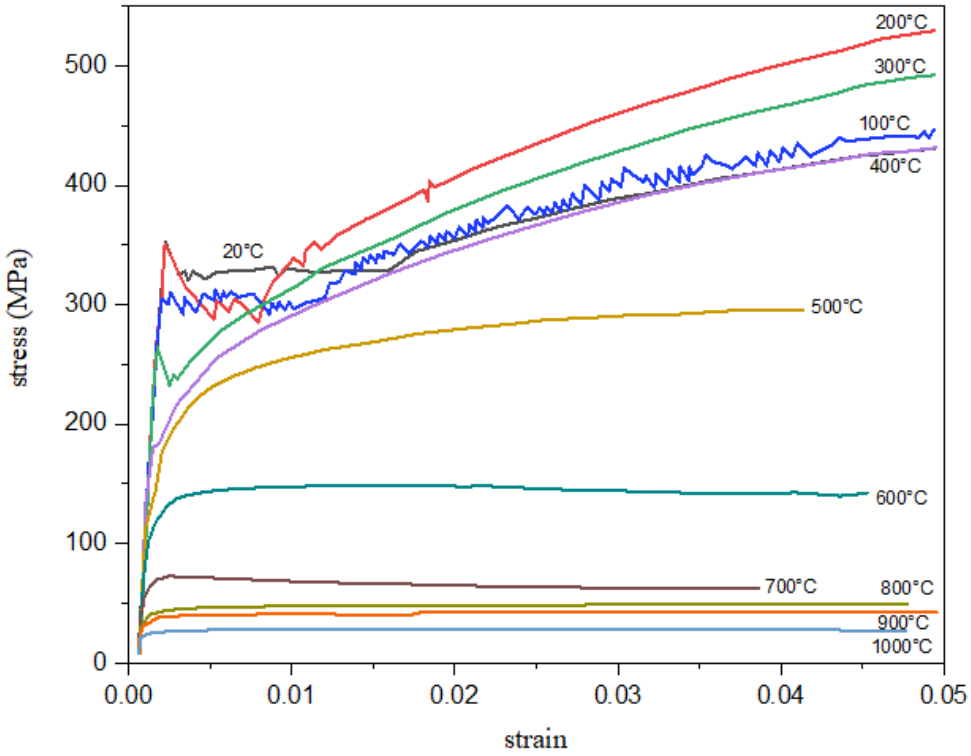

Fig.28. Variation of stress-strain behavior of steel with temperature.

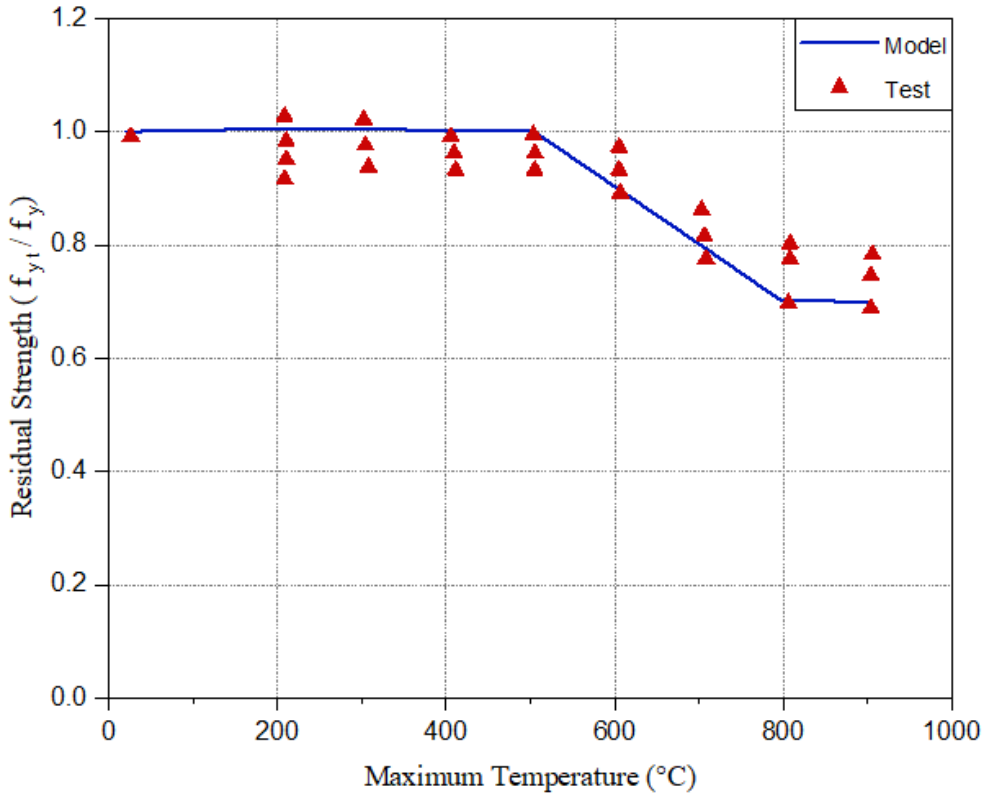

Fig.29. Normalized residual strength of hot rolled reinforcing steel adapted from [178].

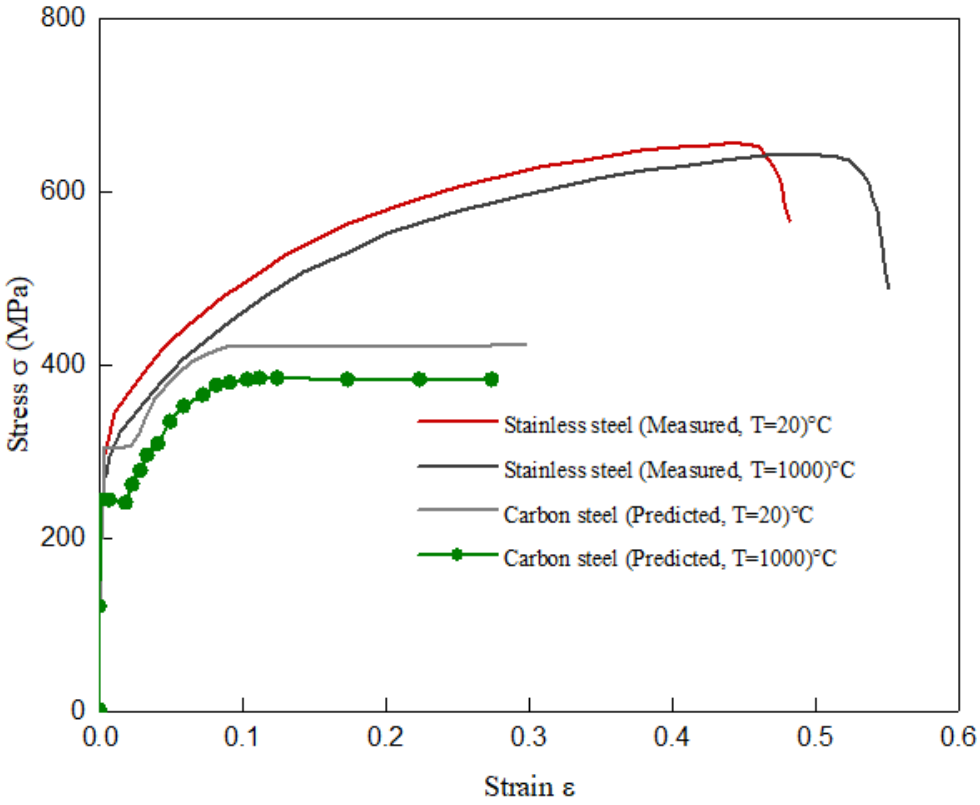

Fig.30. Comparison of post-fire stress-strain curve between stainless steel carbon steel.

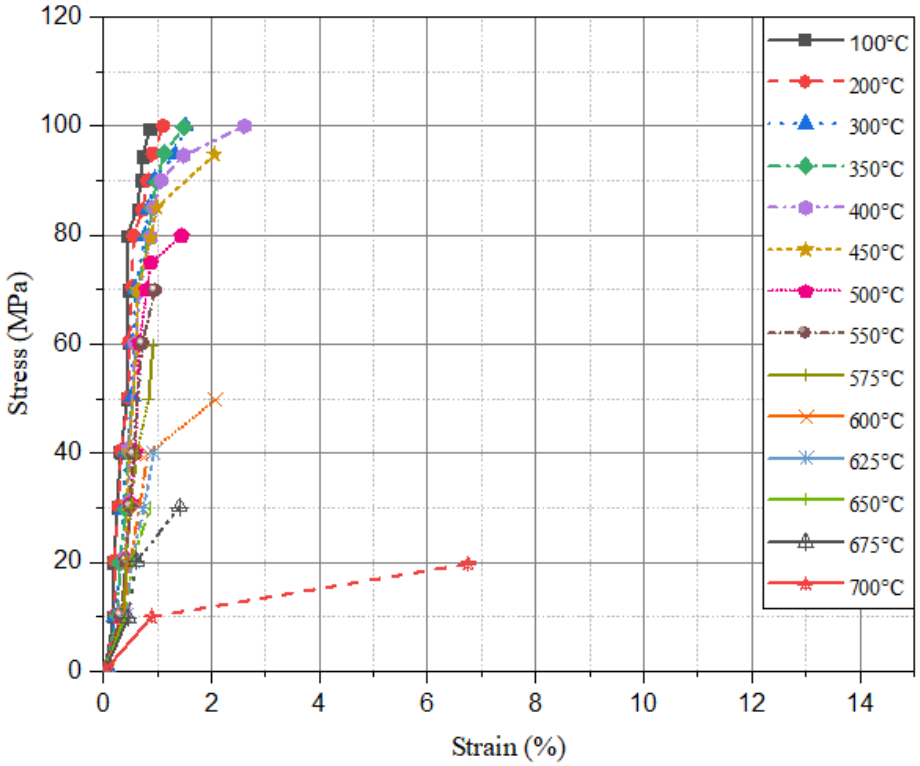

Fig.31. Stress-strain curve of S960 at various temperatures under transient state.

4.1. Analytical solutions local bond slip

This phenomenon considered the effect of the variation of compressive strength of concrete, concrete cover, and temperature on the bond strength degradation. It should be found that the calculation of bond strength based on past studies may be conservative if the concrete cover is relatively small compared with the rebar diameter in which case the concrete cover is more susceptible to splitting failure (Pothisiri, 2012) founded on the antecedent the internal compression from pull-out load (p_p) can be considered to be equilibrated by the pressure resistance of the concrete cover (p_c)

$$p_p = p_c \quad (38)$$

The relationship between the radial pressure of the pull-out load and the bond stress can be expressed as:

$$\tau = p_p cot\alpha \; or \; \tau = p_c cot\alpha \quad (39)$$

Where the effective face angle $\phi = 45°$has been widely adopted to estimate the bond stress at normal temperature (R., 1979) reported that the developed bond stress–slip model has been incorporated into two-node bond-link element within the VULCAN software for analyzing the impacts of bond characteristic on structural behaviors of reinforced concrete structural members in fire (Khalaf, 2016). Based on the theory of elasticity the pressure at the inner surface of uncracked outer part $p_{i,T}$, compressive radial stress σ_r, and the tensile tangential stress $\sigma_{r,T}$ are represented as (Timoshenko S, 1951):

$$\sigma_r = \frac{R_i^2 p_{i,T}}{R_C^2 - R_i^2}\left[1 - \frac{R_C^2}{r^2}\right] \quad (40)$$

$$\sigma_{r,T} = \frac{R_i^2 p_{i,T}}{R_C^2 - R_i^2}\left[1 + \frac{R_C^2}{r^2}\right] \quad (41)$$

For uncracked outer part of the concrete cover the tensile stress $\sigma_{r,T}$ cannot exceed the tensile strength of concrete at elevated temperatures $f_{ct,T}$. According to Eq. (41), $p_{i,T}$ is calculated as:

$$p_{i,T} = f_{ct,T}\frac{R_C^2 - R_i^2}{R_C^2 + R_i^2} \quad (42)$$

Hence, smeared strain of concrete at elevated temperatures $\varepsilon_{u,T}$ increases when temperature increases, as shown in Fig. 37. Therefore, the tensile stress of concrete $\sigma_{t,T}$ can be determined as (Fire design of concrete structures-structural behaviour and assessment. , 2008):

$$\sigma_{t,T} = E_{o,T}\varepsilon_{t,T} \quad (\varepsilon_{t,T} \le \varepsilon_{ct,T}) \quad (43)$$

$$\sigma_{t,T} = \varepsilon_{ct,T}\left[1 - \frac{0.85(\varepsilon_{t,T} - \varepsilon_{ct,T})}{\varepsilon_{1,T} - \varepsilon_{ct,T}}\right] \quad (\varepsilon_{ct,T} < \varepsilon_{t,T} \le \varepsilon_{1,T}) \quad (44)$$

$$\sigma_{t,T} = 0.15 f_{ct,T}\frac{\varepsilon_{u,T} - \varepsilon_{t,T}}{\varepsilon_{u,T} - \varepsilon_{1,T}} \quad (\varepsilon_{1,T} < \varepsilon_{t,T} \le \varepsilon_{u,T}) \quad (45)$$

Where, $\varepsilon_{t,O}$ is the smeared tangential strain of concrete at the rebar interface; $\varepsilon_{ct,T} = f_{ct,T}/E_{o,T}$ is the initial elasticity modulus of concrete at elevated temperatures. Now, the total radial stress at the interface between concrete and steel bar P_T^i equals to the contribution of the uncracked outer part to the radial stress $P_{O,T}^i$ plus the contribution from the cracked inner part in which the softening behaviour of concrete is taken into account. Hence, P_T^i can be calculated as:

$$P_T^i = P_{O,T}^i + \frac{1}{R_s}\int_{R_s}^{R_i} \sigma_{t,T}(r)dr \quad (46)$$

The integration in Eq. (46) can be solved by using Eqs. 43) -(45) as (Wang X, 2003):

$$I = \int_{R_s}^{R_i} \sigma_{t,T}(r)dr = \frac{f_{ct,T}}{\varepsilon_{1,T} - \varepsilon_{ct,T}}\left[(\varepsilon_{1,T} - 0.15\varepsilon_{ct,T})(R_i - R_s) - 0.85 R_i \varepsilon_{ct,T}\, ln\left(\frac{R_i}{R_s}\right)\right]$$

$$(\varepsilon_{ct,T} < \varepsilon_{t,T} \le \varepsilon_{1,T}) \quad (87)$$

$$I = \int_{R_s}^{R_i} \sigma_{t,T}(r)dr = \left[\frac{0.15 f_{ct,T}}{\varepsilon_{1,T} - \varepsilon_{ct,T}}\left(\varepsilon_{u,T}\frac{R_i\varepsilon_{ct,T} - R_s\varepsilon_{1,T}}{\varepsilon_{1,T}} - R_i\varepsilon_{ct,T\,ln}\left(\frac{R_i\varepsilon_{ct,T}}{R_s\varepsilon_{1,T}}\right)\right)\right]$$

$$+\left[\frac{f_{ct,T}}{\varepsilon_{1,T} - \varepsilon_{ct,T}}\left(\left(\varepsilon_{1,T} - 0.15\varepsilon_{ct,T}\right)\frac{R_i\left(\varepsilon_{1,T} - \varepsilon_{ct,T}\right)}{\varepsilon_{1,T}} - 0.85R_i\varepsilon_{ct,T\,ln}\left(\frac{\varepsilon_{1,T}}{\varepsilon_{ct,T}}\right)\right)\right]$$

$$\left(\varepsilon_{1,T} < \varepsilon_{t,T} \le \varepsilon_{u,T}\right) \quad (47)$$

Pothisiri et al. [208] reported that the pressure resistance of concrete in the outer zone, which is in elastic stage, is acquired by substituting the term r_i as shown in Eq. (49). Whereas, the pressure resistance of concrete in the inner zone, which is in the cracked stage, can be computed by integrating the tangential stress over the cracked inner part as shown in Eq. (50).

$$p_{co,T}(r_i) = f_{ct,T}\left(\frac{r_u^2 - r_i^2}{r_u^2 - r_i^2}\right) \quad (49)$$

$$p_{ci,T}(r_i) = \frac{\int_{r_b}^{r_i}\sigma_t(r)dr}{r_b} \quad (50)$$

The pressure resistance, $p_{c\,T}(r_i)$ of the concrete can be computed as a summation of the pressure resistance of the outer zone $p_{co\,T}(r_i)$, and the pressure resistance of the inner zone, $p_{ci\,T}(r_i)$ according to the following pressure equilibrium equation. The variation of the tensile strength of concrete with temperature $\left(f_{ct,T}/f_{ct,20°C}\right)$. (Pothisiri, T., & Panedpojaman, P., 2013) is adopted herein since the properties given by the Eurocodes significantly differ from other researchers and the estimated of the tensile strength obtained from the Eurocodes is zero for temperatures higher than 600 °C (Bazant P, 1987). studied the tensile stress-strain relation of concrete based on the work of Pothisiri and Panedpojaman are adopted herein. The bond-slip relationships at normal temperature and elevated temperatures obtained by using the proposed model are compared with the previous experimental results as shown in Figs. 8–9. In some cases of the comparison (Pothisiri T, 2012). Eq. (51) considers plain rebar bond strength, whereas Eq. (52) considers deformed rebar bond strength, respectively. In these equations, the influences of concrete cover, bar diameter, embedment length, and compressive strength (at the curing age) parameters are considered (Aslani F. &., 2013).

$$\tau_{max,20} = \left(0.7\left(\frac{c}{d_b}\right)^{0.6} + 4\left(\frac{d_b}{l_d}\right)\right)\left(f_c'\right)^{0.23} \quad (51)$$

$$\tau_{max,20} = \left(0.679\left(\frac{c}{d_b}\right)^{0.6} + 3.88\left(\frac{d_b}{l_d}\right)\right)\left(f_c'\right)^{0.55} \quad (52)$$

Where, d_b is the diameter of the steel bar, l_d is the embedded length of the steel bar, f_c' is the compressive strength of the concrete, and c is the concrete cover. Proposed bond strength models are related to compressive strength.

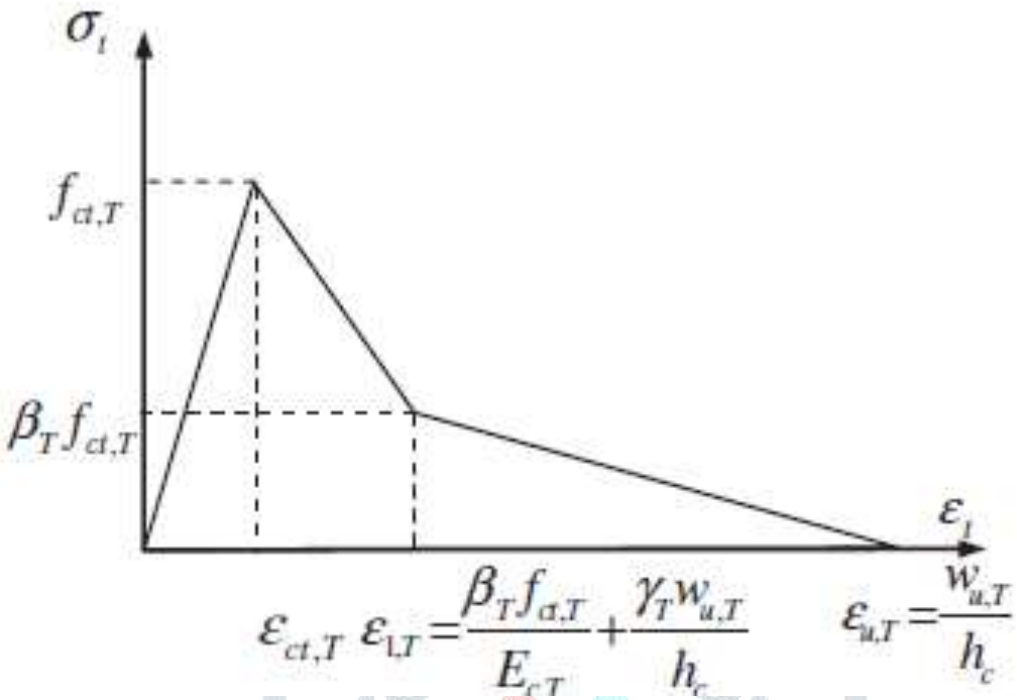

(32) Tensile stress–strain relationship

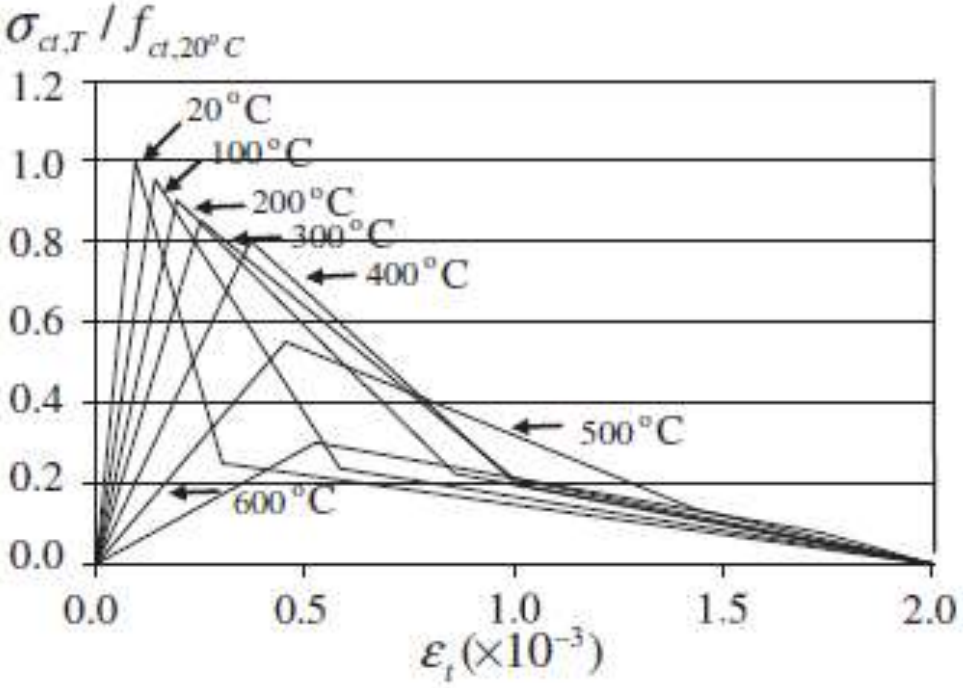

(b) Variation of normalized tensile stress-strain relationships with temperature.

Fig. 33. Tensile stress–strain relationship for concrete at elevated temperatures. (Wang X, Liu X., 2003; code., 1993; Panedpojaman P, 2010; Pantazopoulou SJ, 2001).

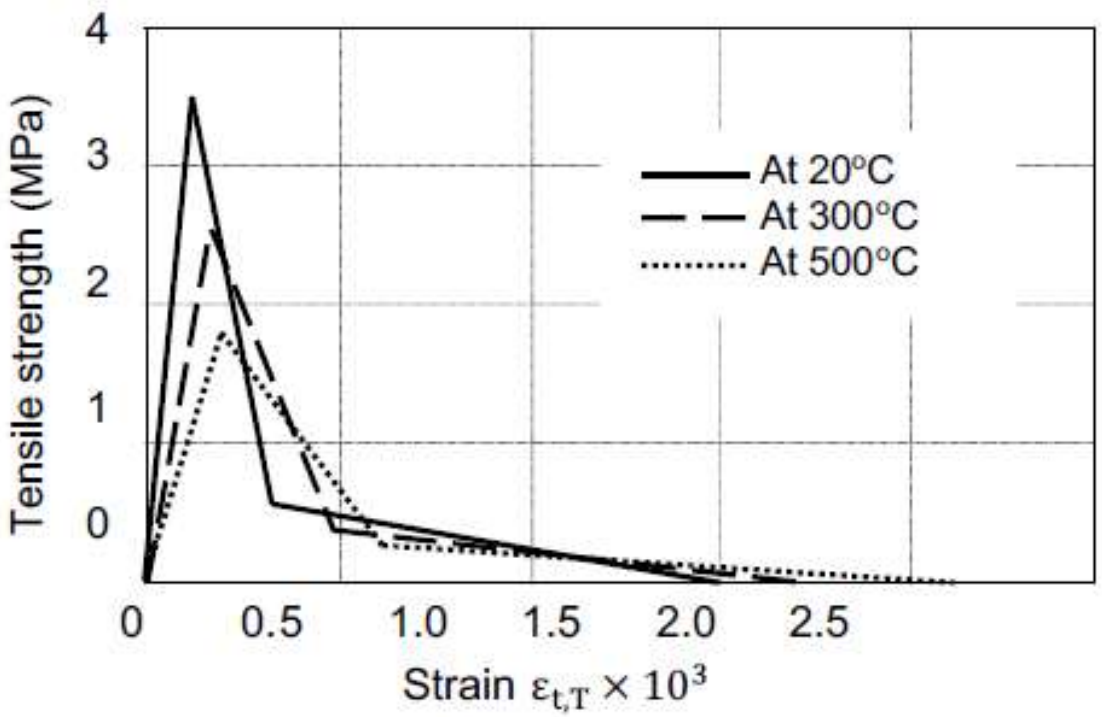

Fig. 34. Concrete tensile stress–strain curves at different temperatures. (Fire design of concrete structures-structural behaviour and assessment., 2008).

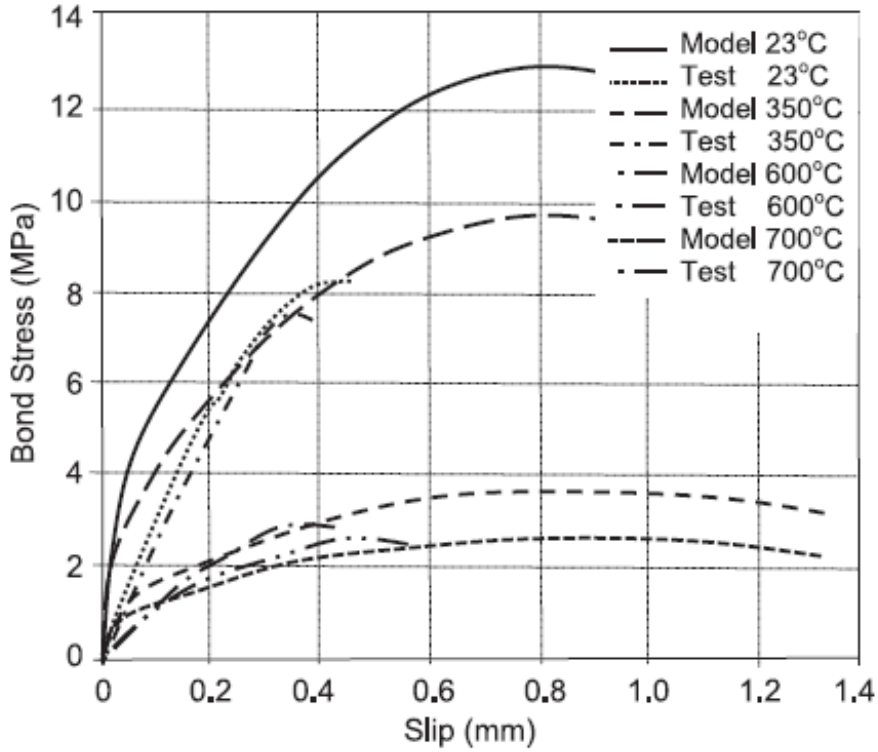

Fig.35. Comparison of predicted and measured bond stress-slip curves at elevated temperatures. (Haddad RH, Al-Saleh RJ, Al-Akhras NM., 2008).

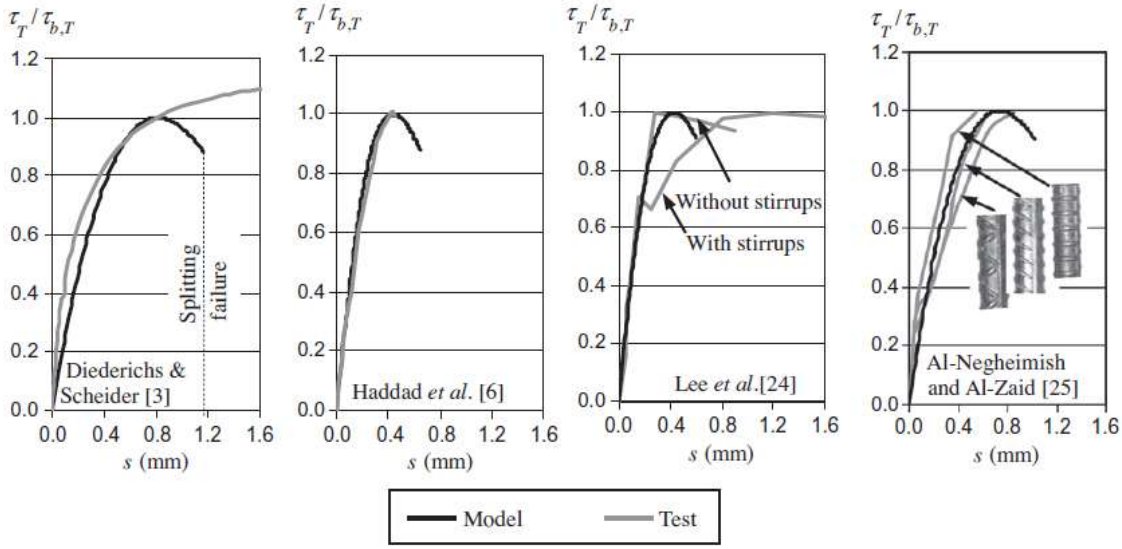

Fig. 36. Comparison between the bond stress–slip relationships obtained by the proposed method and the test results for the normal-temperature case. (Pothisiri T, Panedpojaman P., 2012).

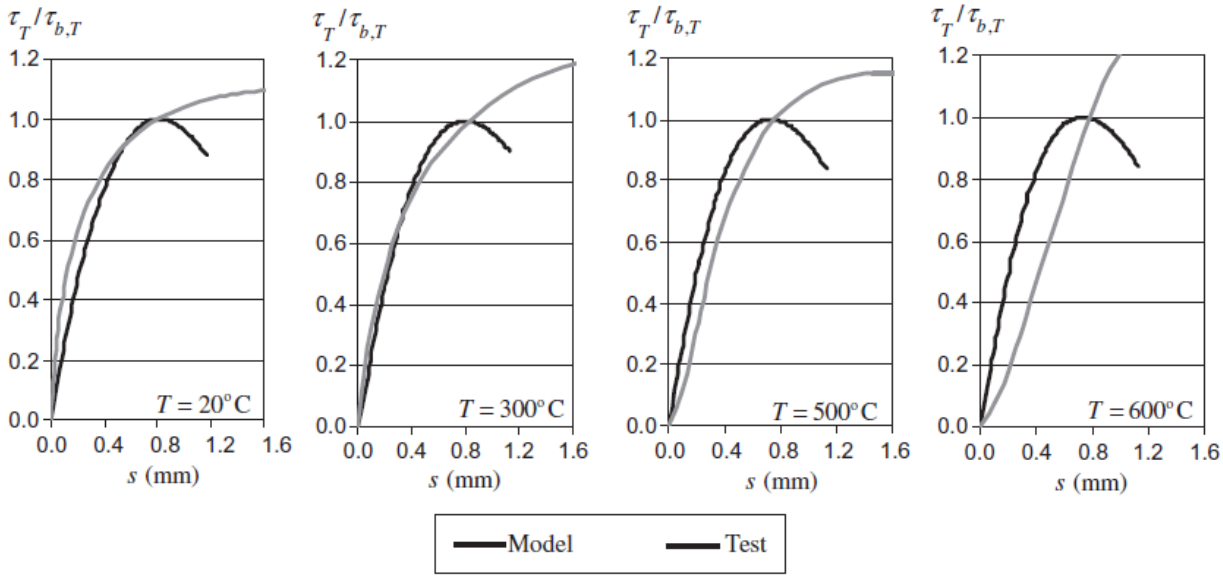

Fig.37. Comparison between the bond stress–slip relationships obtained by the proposed method and the test results of (Diederichs U, Schneider U., 1981).

4.2. Bond-slip relationship

Numerous researchers investigated the bond-slip relationship of residual bond behavior of concrete and steel at different temperatures. The details bond-slip relationship presents the various parameters on the bond behavior of concrete and steel, including the elevated temperatures. Such as the bond-slip relationship test results between the steel rebar and concrete at elevated temperatures to the different specimens, loading history and are updated every time reserved the relationship showing in equations 56 Bond-slip relationship between the internal reinforcement grouting, CEB- FIP Model Code 90. And all factors that influence bond-slip performance. The results showed that the

marked decreases in the residual compressive and steel-concrete bond under high temperatures among dramatic changes in bond stress–free-end slip trend behavior. The use of fibers minimized the damage in steel-concrete bond under elevated temperatures and hence the decrease in bond strength. Specimens that included hooked steel fibers achieved the most significant bond resistance against elevated temperatures observed, in sequence, by those prepared with the mixture of hooked and brass-coated steel, the mixture of hooked steel and polypropylene, and brass-coated steel fibers. Statistical models for bond stress versus free-end slip and bond strength versus exposure temperature developed. These showed the best agreement with the trend behavior of present test data. Post-heating behavior of the concrete-steel bond has been studied over the past 50 years utilizing two types of bond test specimens, defined in ASTM, and RILEM test methods (Haddad, 2008).The results carried out in the one-dimensional (1D) bond-slip relations for corroded reinforcement has been developed and is presented in this study. The equilibrium equation along a reinforcement bar is

$$\frac{\pi \times d^2}{4} \times \frac{d\sigma}{dx} - \pi \times d \times \tau = 0 \quad (53)$$

Where, d is the rebar diameter, σ is the stress in the rebar, and τ is the bond stress (Lundgren, 2012). studied the bond-slip behavior of reinforcing bars in well-confined concrete under monotonic and low-cycle fatigue loads. Three to researched the bond-slip behavior to each of the 35, 43, and 57-mm bar sizes, and the fourth to study the effect of the compressive strength of concrete on the bond strength. Over-all of 22 specimens were tested, of which eight subjected to monotonic loading and 14 to cyclic loading. The total dropped resistance τ_{red} at any time is expected to be the sum of the worsened bearing resistance, $\tau_{b,red}$, and the deteriorated friction resistance, τ_f, red. The reduction of the two resistance components is controlled by two damage parameters that depend on the loading history and are updated every time the load reversed — the relations are showing in Equation 54 (R. Eligehausen, 1983; Murcia-Delso, 2011).

$$\tau_{red} = \tau_{b,red} + \tau_{f,red}$$
$$\tau_{b,red} = (1 - d_b)\tau_b \quad (54)$$
$$\tau_{b,red} = (-d_f)\tau_f$$

investigated that the analytical model developed for the bond-slip mechanism between steel rebar and concrete at elevated temperatures. The model without the standardized bond stress–slip relationship The bond-slip relationships at standard elevated temperatures achieved with the proposed model with the previous test results, in some cases of the comparison, the investigational slips probably more significant than the modeling results due to the combination (Pothisiri, T., & Panedpojaman, P., 2013) proposed that the bond-slip relationship for open bars are still not well known, and existing experimental expressions are institute not to take into account all the factors that influence bond-slip performance. Based on the experimental results, new experimental expressions proposed for the limitations adopted in one of the more recent bond-slip models for open bars available in the literature (Melo, 2015). The result recommended that the increase of age, the bond strength between steel bar and grouting material is increasing piecemeal, the increased speed piecemeal slowed down after 20 days. The bond-slip relationship between the internal reinforcement grouting material in the sleeve by the indirect method and the bond-slip relationship between the sleeve grouting material will be showed as follow-up work (Wang J. C., 2016).thus, information on permeability of model for predicting the bond-slip between the concrete and steel reinforced bar at elevated temperatures. In instruction to determinate the bond-slip relationship, the maximum bond-slip S_{max} established from the bond stress–slip model in CEB- FIP Model Code 90, the bond-slip of the rebar can be determined by resolute the maximum slip S_{max} at the maximum bond stress point τ_{max}. The S_{max} equals to 0.6 mm for splitting failure at the concrete cover $C = d_b$, and 1.0 mmm for pull-out failure at the concrete cover $C \geq d_b$ in excellence bond conditions (Khalaf, J., Huang, Z., & Fan, M., 2016; 1990., 1991).

$$S_{max} = 0.6 + 0.1 \times \left(\frac{C}{d_b} - 1\right) \quad (55)$$

The test results showed that the progressive increase of residual slip considered the bond behavior under repeated loading. The slip increase became more diphthongized when the stress level had increased. Through a systematic evaluation of the test data, a model for the bond stress-slip relationship under repeated loading has proposed. To consider the slip increase under repeated loading:

$$S_n = S_o(1 + K_n), K_n = (1 + n)^b - 1 \quad (56)$$

Where, s_o is the initial slip, k_n is the slip coefficient depending on the number of loading cycles and b = 0.107. The value of power b varies with the test results of different authors (Lin, 2017). investigated that the bond-slip curve divided into two segments, which considered through two, not the same mechanical models. The slip is showed as displacement boundary conditions into the model, which is the main innovation of this case. The Comparison between calculated values and test results shows that the theoretical model can reasonably predict the local bonding problems with different steel bar diameters and concrete strength grades (Zhao W. &., 2018).

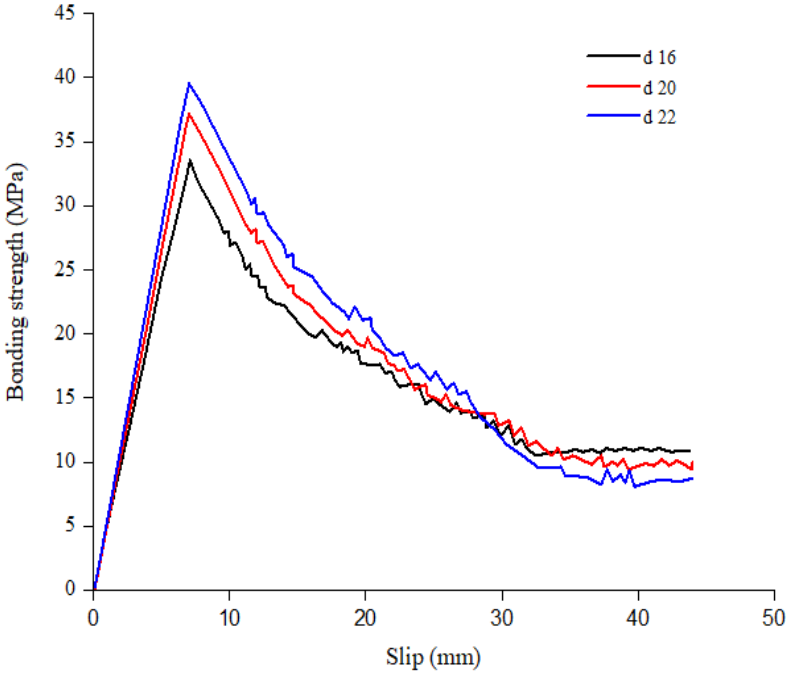

Fig.38. the bond-slip curve of twentieth day Updated from (Wang, J. C., Zhou, J. H., Pan, M. X., & Zhang, D. Y., 2016)

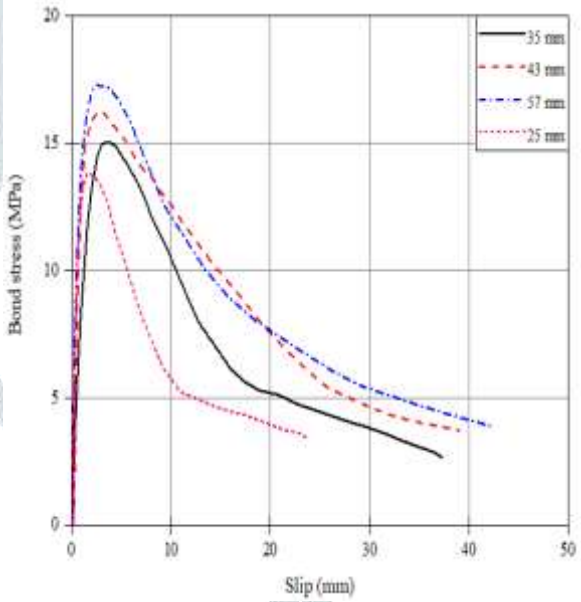

Fig.39. Monotonic bond stress vs. slip relations obtained from tests (the curve for 25-mm bars Updated from (R. Eligehausen, E.G. Popov, V.V. Bertero,, 1983).

5. Conclusions

Based on the review of several papers on the Residual mechanical and bond properties of concrete and steel after exposure to elevated temperatures, the key findings are gained as bellow:

- Descent possessions of mechanical concrete happens at the high temperature.
- Throughout the high temperature contact, concrete experiences a sequences of chemical and physical variations, such as collapses of hydration products, water vanishing, and totals, coarsening of microstructure and increase of absorbency. Such kind of variations are measured to be accountable for the weakening of mechanical properties of concrete in the high temperature.
- The high-temperature compressive strength, tensile stregth, and modulus of resistance weaken with the growing temperature variety. Although, the residual mechanical properties are considered in the different stages of temperature.

- Steel fibers not only progress the spalling confrontation but also recover the RPC mechanical properties too in the room temperature as well as the high temperature. The amount of steel fibers to avoid spalling growths with the increase of Regional Prime Contracts compressive strength and with the association can be uttered as an advocate function.
- Commonly, concrete mechanical behavior under the high temperature is better rather than that concrete high temperature. As for rebar, the reflection of contraries.
- Emission of Silica does not have important effect on the excruciating tensile strength of concrete. Fume of Silica appeared to have pronounced influence on flexural strength in evaluation with splitting tensile strength. Flexural strengths, even very high percentages of silica fume meaningfully developed the strength. Although, it was originated that there was a stable increase in the flexural strength with the increase of silica fume.

According to the review of RPC in and after the high temperature, the future studies are recommended, the actual experiment in the high temperature and fire confrontation researches of concrete is to examine the performance of structure under the high temperature and fire. Narrow studies works have been stated for full scale structural members of RPC under the high temperature. Additional study is essential for variables such as dosage of fibers, load level, heating rate, duration of heating and structural size member for more and complete comprehension of structural performance under high temperature and fire.

References

(Sherif Yehia., e. a. (2011). RECOMMENDED CONCRETE PROPERTIES FOR HIGH STRENGTH STEEL REINFORCEMENT. . Balatonfured, Hungary. : Conference: 7th CCC CONGRESS BALATONFURED at: .

1990., C.-F. m. (1991). Final draft, committe euro-international du beton. Bulletin d'information No. , 203-205; .

3:, E. (2005). European Committee for Standardization. EN1993-1-2. Eurocode 3: Design of Steel. ,General Rules, Structural Fire Design., 1,2.

4:, E. (2005). European Committee for Standardization. EN1994-1-2. Eurocode 4: Design of Composite Steel and Concrete Structures, Part 1-2: General Rules,. Structural Fire Design. European Committee for Standardization.

A. W. Hussein. (2009). . (2009). Ultimate Strength of Intact and Damaged Bulk Carriers. . 13th Congressof Intl. Maritime Assoc. of Mediterranean IMAM , 12-15 Oct. .

Abrams, M. S. (1971). Compressive strength of concrete at temperatures to 1600F. ACI Special Publication, 25(14359/17331), 33–58.

ACI 318-08. (2007). Building Code Requirements for Structural Concrete andCommentary. Farmington Hills:American Concrete Institute, ACI 318-08:.

Ahmad, S. S.-H. (2014). Effects of Key Factors on Compressive and Tensile Strengths of Concrete Exposed to Elevated Temperatures. Arabian Journal for Science and Engineering, , 39(6), 4507–4513.

Ahmed, M. M. (2016). A study of factors affecting the flexural tensile strength of concrete. . Journal of King Saud University - Engineering Sciences, , 28(2), 147–156.

Al-Zube, L. S. (2018). The elastic modulus for maize stems. . Plant Methods, 14(1). .

Anderberg Y, T. S. (1976). Stress and deformation characteristics of concrete at high temperatures: 2 experimental investigation and material behaviour model. : Lund Institute of Technology;, 54.

Anthony Nkem Ede, O. M. (2014). Experimental Investigation of Yield Strengths of Steel Reinforcing Bars Used in Nigerian Concrete Structures. . International Journal of Scientific & Engineering Research,, 2229-5518.

Arioz, O. (2007). Effects of elevated temperatures on properties of concrete. Fire Safety Journal, 42(8), 516–522.

Aslani, F. &. (2013). Predicting the bond between concrete and reinforcing steel at elevated temperatures. Structural Engineering and Mechanics,, 48(5), 643–660.

Aslani, F. a. (2014). High Strength Polypropylene Fibre Rein forcement Concrete at High Temperature," . Fire Technology, , 1229-1247.

ASTM. (2014). Standard Test Method for Fundamental Transverse, Longitudinal, and Torsional Resonant Frequencies of Concrete Specimens,. ASTM International, West Conshohocken, PA, C215-14,.

ASTM. (2016.). Standard Test Method for Pulse Velocity Through Concrete,. ASTM International, West Conshohocken, C597-16, , PA, .

ASTMD. (1992). Standard test method for apparent tensile strength of ring or tubular plastics and reinforced plastics by split disk method. . Annual Book of ASTM Standards, , 15.03.

Bamonte, P. &. (2012). High-Temperature Behaviour of Concrete in Tension. . Structural Engineering International, , 22(4), 493 499.

Barnett, M. R. (2006). A semi analytical Sachs model for the flow stress of a magnesium alloy. Metallurgical and Materials Transactions A: Physical Metallurgy and Materials Science, , 37(7), 2283–2293.

Bayatfar, A. K. (2014). Residual ultimate strength of cracked steelunstiffened and stiffened plates under longitudinal compression. . Thin-Walled Structures, , 84, 378–392.

Bayraktar, H. H. (2004). Comparison of the elastic and yield properties of human femoral trabecular and cortical bone tissue. Journal of Biomechanics, 37(1), 27–35.

Bazant P, C. J. (1987). Stress-induced thermal and shrinkage strains in concrete. . J Eng Mech ASCE , 113(10):1493–511.

Behnood, A. &. (2009). Comparison of compressive and splitting tensile strength of high-strength concrete with and without polypropylene fibers heated to high temperatures. . Fire Safety Journal, 44(8), 1015–1022.

Brussels. (1991). ENV 1992-1-1. (1991).Eurocode 2:Design of concrete structures - Part 1: General rules and rules for buildings. CEN.

BS 8110. Structural Use of Concrete, P. 1. (1997). Code of Practice for Design and Construction,. London, UK: British Standards Institution,.

Buchanan, A. M. (2004). The effect of stress-strain relationships on the fire performance of steel beams. . Engineering Structures,, 26(11), 1505–1515.

Bulletin. (2010). Model Code 2010 . Switzerland: The International Federation for Structural Concrete, 66.

Burssles:. (2004). EN 1992-1-1: General rules and rules for buildings. Comité Européen de Normalisation.

C. R. Cruz, “. (n.d.). Elastic properties of concrete at high temperatures. Journat of the PCA Research and Development Laboratories,, 37–45, 1966.
C.S. Poon, Z. S. (2004). Compressive behavior of fiber reinforced high-performance concrete subjected to elevated temperatures. Cement and Concrete Research , 34 , 2215–2222.
CARREIRA, D. C. (1985). “Stress-strain relationship for plain concrete in compression”, . ACI Journal, , 797-804,.
CEN., B. (2004). Design of concrete structures - Part 1-1: General rules and rules for buildings. . Eurocode 2: , EN 1992-1-1. .
Chen, J. Y. (2006). Behavior of High Strength Structural Steel at Elevated Temperatures. Journal of Structural Engineering, , 132(12), 1948–1954.
Chiorean C.G., S. M. (2019). Ultimate Strength Analysis of Steel-Concrete Cross-Sections at Elevated Temperatures. pecial Session CC27 CIVIL-COMP 2019 Computational Efficient Models for Non-Linear Inelastic Analysis of Building Frameworks, 03(07),2-9,2019.
code., C.-F. m. (1993). CEB Bulletin information no. . Committee Eurointernational Du Beton. Thomas Telford;, 213/214.
Comparative analysis of dependence of the elastic modulus of concrete on its composition. . (2018). Materials Structures Technology, , 1(1), 1–9.
Czujko, N. A. (2018). ULTIMATE STRENGTH Proceedings of the Image International Ship and Offshore Structures Congress .ISSC 2018 committee III.I: . This article is published online with Open Access by IOS Press and distributed under the terms of the Creative Commons Attribution Non- Commercial License 4.0 (CC BY-NC 4.0). .
Diederichs U, Schneider U. (1981). Bond strength at high temperatures. . Mag Concr Res , 33(115):75–84.
Dr. M.L. Kaminski., e. a. (2000). TECHNICAL COMMITTEE III.1 ULTIMATE STRENGTH. . 14th INTERNATIONAL SHIP AND OFFSHORE STRUCTURES CONGRESS , 2-6 OCTOBER.
Drzymała, T. J.-R. (2017). Effects of High Temperature on the Properties of High-Performance Concrete (HPC). . In Procedia Engineering Elsevier Ltd, (Vol. 172, pp. 256–263).
ECCS Technical Committee 3. (1989). European Convention for Construction Steelwork. Calculation for Fire Resistance of Composite Structures. . Technical Note No., 55.
Elghazouli, A. Y. (2009). Experimental evaluation of the mechanical properties of steel reinforcement at elevated temperature. . Fire Safety Journal, 44(6), 909–919. .
ENV. (1991). Eurocode 2: Design of Concrete Structures— Part 1: General Rules and Rules for Buildings, . European Committee for Standardization, Brussels,, 1992-1-1. .
Ervine, A. G. (2011). Thermal Propagation through Tensile Cracks in Reinforced Concrete. . Journal of Materials in Civil Engineering, , 24(5), 516–522.
Eurocode 2:1992-1-2:2004. (2004). Design of concrete structures - Part 1-2: General rules - Structural fire design. uk: Eurocode 2, BS EN 1992, 97.
Falliano, D. D. (2019). . Compressive and flexural strength of fiber-reinforced foamed concrete: Effect of fiber content, curing conditions and dry density. Construction and Building Materials,, 198, 479–493.
Fang., E. S.-S. (2014). Direct Tensile Behavior of Normal-Strength Concrete at Elevated Temperatures. . ACI Materials Journal, 111-M57.
Fire design of concrete structures-structural behaviour and assessment. (2008). Fib Fédération internationale du béton – building, fireproof, fib bulletin , 46;.
Folagbade Olusoga Peter ORIOLA, G. M. (2017). Estimating the shear strength of concrete with coarse aggregate replacement. . Leonardo Electronic Journal of Practices and Technologies. , ISSN 1583-1078, .
Fu, Y. F. (2005). Stress–strain behaviour of high-strength concrete at elevated temperatures. Magazine of Concrete Research, 57(9), 535–544.
Fu-Ping Cheng, V. K.-C. (2004). Stress-Strain Curves for High Strength Concrete at Elevated Temperatures. Journal of Materials in Civil Engineering, 16(1), 84–90.
Gadea, J. M. (2019). Numerical Simulation of Steel Reinforced Concrete (SRC) Joints. . Metals,, 9(2), 131. .
Gai-Fei Peng, S.-H. B.-Q.-L.-C. (2008). Effect of thermal shock due to rapid cooling on residual mechanical properties of fiber concrete exposed to high temperatures . Construction and Building Materials,, 22(5), 948–955.
Gandomi, A. H. (2010). Formulation of elastic modulus of concrete using linear genetic programming. Journal of Mechanical Science and Technology,, 24(6), 1273–1278.
Gao, F. T. (2018). Ultimate strength of tubular T-joints reinforced with doubler plates after fire exposure. . Thin-Walled Structures,, 132, 616–628.
Gul, M. B. (2014). Study of modulus of elasticity of steel fiber reinforced concrete. . International Journal of Engineering and Advanced Technology, 3(4), 304–309.
Haddad RH, Al-Saleh RJ, Al-Akhras NM. (2008). Effect of elevated temperature on bond between steel reinforcement and fiber reinforced concrete. . Fire Saf J, 43:334–43.
Haddad, R. H.-S.-A. (2008). Effect of elevated temperature on bond between steel reinforcement and fiber reinforced concrete. . Fire Safety Journal, , 43(5), 334–343.
Harish Kumar N R, J. L. (2015). EVALUATION OF IN-PLANE SHEAR STRENGTH IN SCC USING INCLINED. International Research Journal of Engineering and Technology (IRJET). , 2395-0072.
Heintze, S. D. (2017). Laboratory mechanical parameters of composite resins and their relation to fractures and wear in clinical trials—A systematic review. Dental Materials.
Hopcroft, M. A. (2010). What is the Young’s modulus of silicon? Journal of Microelectromechanical Systems, , 19(2), 229–238.
Hou, X. A. (2017). Evaluation of residual mechanicalproperties of steel fiber-reinforced reactive powder concrete after exposure to high temperature using nondestructive testing. In Procedia Engineering , (Vol. 210, pp. 588.
Husem, M. (2006). The effects of high temperature on compressive and flexural strengths of ordinary and high-performance concrete. Fire Safety Journal, 41(2), 155–163.

Ignasi Fernandez, J. M. (2015). Corrosion effects on the mechanical properties of reinforcing steel bars. Fatigue and r–e behavior. . Construction and Building Materials, 772–783.
Ika Bali, a. P. (2016). SHEAR STRENGTH OF REINFORCED CONCRETE WALLS WITH BOUNDARY MEMBER. . Seminar Nasional Teknologi dan Sains (SNTS) , 23-24 .
J. K. Paik, K. B. (2009). Ultimate Strength. 17th INTERNATIONAL SHIP AND OFFSHORE STRUCTURES CONGRESS . ISSC Committee III.1: , (pp. 16-21 AUGUST). SEOUL, KOREA.VOLUME 1.
Janda, R. R. (2006). The effects of thermocycling on the flexural strength and flexural modulus of modern resin-based filling materials. . Dental Materials,, 22(12), 1103–1108.
Jang. I.Y., P. H. (1996). A Proposal of Elastic Modulus Equation for High-Strength and Ultra- High-Strength,. KCI, 213-222.
Jeom KeePaik. (2008). Residual ultimate strength of steel plates with longitudinal cracks under axial compression–experiments. . Ocean Engineering 35, 1775–1783.
Jingming Cai, J. Y. (2015). Mechanical behavior of steel-reinforced concrete-filled steel tubular (SRCFST)columns under uniaxial compressive loading. Thin WalledStructures, 97(2015)1–10.
Jose-Miguel Albaine, M. P. (2012). Shear Strength of Reinforced Concrete Beams per ACI 318-02. PDH Online | PDH Center. PDH online Course, S153 (4 PDH).
Júnior, L. Á., Borges, V. E., Danin, A. R., Machado, D. V., Araújo, D. d., Deb, M. K., & Rodrigues, P. F. (2010). Stress-strain curves for steel fiber reinforced concrete in compression. . In 65th ABM International Congress, 18th IFHTSE Congress and 1st TMS/ABM International Materials Congress , (Vol. 7, pp. 5447–5454).
K.J.N. Maclean, L. B. (2008). Post-fire deterioration and prestress loss in steel tendons used in post-tensioned slabs,. ACI Spec. Publ., 5147–174.
Kaklauskas, G. &. (2001). Stress-strain relations for cracked tensile concrete from RC beam tests. Journal of Structural Engineering New York, N.Y.,, 127(1), 64–73.
Karakoç, M. B. (2013). Effect of cooling regimes on compressive strength of concrete with lightweight aggregate exposed to high temperature. Construction and Building Materials, 41, 21–25.
Kee Paik, J. (2008). Ultimate strength of perforated steel plates under combined biaxial compression and edge shear loads. Thin-Walled Structures,, 46(2), 207–213. .
Khalaf, J. H. (2016). Analysis of bond-slip between concrete and steel bar in fire. . Computers and Structures, 162, 1–15.
Khalaf, J., Huang, Z., & Fan, M. (2016). Analysis of bond-slip between concrete and steel bar in fire. . Computers and Structures, , 162, 1–15.
Khaliq, W. &. (2011). Effect of high temperature on tensile strength of different types of high-strength concrete. . ACI Materials Journal, , 108(4), 394–402.
Khoathane, M. C. (2008). Hemp fiber-reinforced 1-pentene/polypropylene copolymer: The effect of fiber loading on the mechanical and thermal characteristics of the composites. Journal of Reinforced Plastics and Composites, 27(14), 1533–1544.
Kodur, V. D. (2010). High-temperature properties of steel for fire resistance modeling of structures. Journal of Materials in Civil Engineering,, 22(5), 423–434.
Kodur, V. K. (2008). High-temperature properties of concrete for fire resistance modeling of structures. ACI Materials Journal, 105(5), 517–527.
Kodur, V. K. (2016). An approach for evaluating residual capacity of reinforced concrete beams exposed to fire. . Engineering Structures,, 110, 293–306.
Kodur, V. W. (2004). Predicting the fire resistance behavior of high strength concrete columns. Cement & Concrete Composites, 26, 141-153.
Kodur., V. (2014). Properties of Concrete at Elevated Temperatures. ISRN Civil Engineering, 10.1155, 468510, 15.
Köksal, F. A. (2008). Combined effect of silica fume and steel fiber on the mechanical properties of high strength concretes. . Construction and Building Materials,, 22(8), 1874–1880.
Korentz, J. (2010). The effect of yield strength on inelastic buckling of reinforcing bars. . Mechanics and Mechanical Engineering, , 14(2), 247–255.
Korentz, J. (2010). The effect of yield strength on inelastic buckling of reinforcing bars. . Mechanics and Mechanical Engineering,, 14(2), 247–255.
Ku, H. W. (2011). A review on the tensile properties of natural fiber reinforced polymer composites. Composites Part B: Engineering,, 42(4), 856–873.
Kusakin, P. B. (2017). On the effect of chemical composition on yield strength of TWIP steels. . Materials Science and Engineering A, , 687, 82–84.
Lahoti, M. T. (2019). A critical review of geopolymer properties for structural fire-resistance applications. Construction and Building Materials, 06.076.
Lam, E. S. (2014). Direct tensile behavior of Normal-Strength concrete at elevated temperatures. . ACI Materials Journal, , 111(6), 641–650.
Lam, L. &. (2003). Design-oriented stress-strain model for FRP-confined concrete. . In Construction and Building Materials, (Vol. 17, pp. 471–489).
Lau, A. A. (2006). Effect of high-temperatures on high-performance steel fiber reinforced concrete. Cement and Concrete Research, 36, 1698 – 1707.
Li, H. Y. (2012). Experimental research on compressive strength degradation of reactive powder concrete after high temperature. Journal of Harbin Institute of Technology, 44(4)(03676234), 0017-06.
Lin, H. Z.-W. (2017). The bond behavior between concrete and corroded steel bar under repeated loading. Engineering Structures, , 140, 390–405.
Liu, F. G. (2014). Post-fire behaviour of reinforced concrete stub columns confined by circular steel tubes. . Journal of Constructional Steel Research,, 102, 82–103.

Lodi., M. M. (2017). Mechanical properties of low-strength concrete at exposure to elevated temperature. Journal of Structural Fire Engineering, , DOI: 10.1108/JSFE-11-2016-0017.
Lu, J. L. (2016). Experimental investigation into the post-fire mechanical properties of hot-rolled and cold-formed steels. . Journal of Constructional Steel Research,, 121, 291–310.
Lu, J. L. (2017). Experimental investigation of the residual mechanical properties of cast steels after exposure to elevated temperature. . Construction and Building Materials, , 143, 259–271.
Lubna S. Ben Taher, M. S. (2013). Variability in Yield Strength and Elongation of Reinforcing Steel Bars. . Conference Paper ·.
Lundgren, K. K. (2012). Analytical model for the bond-slip behaviour of corroded ribbed reinforcement. . Structure and Infrastructure Engineering,, 8(2), 157–169.
Lundgren, K., Kettil, P., Hanjari, K. Z., Schlune, H., & Roman, A. S. S. (2012). Analytical model for the bond-slip behaviour of corroded ribbed reinforcement. . Structure and Infrastructure Engineering,, 8(2), 157–169.
Luo, B. F. (2012). ompressive properties of cube for reactive powder concrete with polypropylene fibers at elevated temperature. Journal of Harbin Institute of Technology, 44(12)(03676234), 1–7.
Ma, Q. G. (2015). Mechanical properties of concrete at high temperature-A review. Construction and Building Materials. , 93 (2015) 371–383.
Mahendran, M. (1996). The modulus of elasticity of steel - Is it 200 GPa? In International Specialty Conference on Cold-Formed Steel Structures: . Recent Research and Developments in Cold-Formed Steel Design and Construction , (pp. 641–648).
Melo, J. R. (2015). Experimental study of bond–slip in RC structural elements with plain bars. . Materials and Structures/Materiaux et Constructions,, 48(8), 2367–2381.
Mereen Hassan Fahmi Rasheed, S. E. (2018). EFFECT OF STEEL REINFORCEMENT ON THE MINIMUM DEPTH-SPAN RATIO. . 4th International Engineering Conference on Developments in Civil & Computer Engineering Applications , 2409-6997.
Mirza, S. A. (1979). Variability of Mechanical Properties of Reinforcing Bars," . Journal of the Structural Division, ASCE, , 921-937.

Mr. Chandrashekharamurthy H. K, D. P. (2019). Shear Strength, Compressive Strength and Workability Characteristics of Concretes Reinforced with Steel Fibres. International Journal of Engineering Research & Technology (IJERT). , 2278-0181.
Mr. Prasad V, D. P. (2019). Comparative Study on Shear Strength of Steel Fibre reinforced Self-Compacting and Normal Cement Concrete of Grades M30 and M60. International Journal of Engineering Research & Technology (IJERT), 2278-0181.
Muhammad Abid, X. H. (2017). High temperature and residual properties of reactive powder. Construction and Building Materials , 147 , 339–351.
Murcia-Delso, J. S. (2011). Modeling the bond-slip behavior of confined largediameter reinforcing bars. 3rd International Conference on Computational Methods in Structural Dynamics and Earthquake Engineering: An IACM Special Interest Conference, Programme. In ECCOMAS Thematic Conference - COMPDYN 2011: .
Nakai, T. M. (2006). Effect of pitting corrosion on the ultimate strength of steel plates subjected to in-plane compression and bending. . Journal of Marine Science and Technology, , 11(1), 52–64.
Neves I, R. J. (1996). Mechanical properties of reinforcing and prestressing steels after heating. J Mater Civ Eng , 8:189–94.
Noguchi, T. T. (2009). A practical equation for elastic modulus of concrete. . ACI Structural Journal, , 106(5), 690–696.
Oad, R. (2018). Effect of steel fibres on the compressive and flexural strength of concrete. I. nternational Journal of ADVANCED AND APPLIED SCIENCES,, 5(10), 16–21. .
Paik, J. K. (2005). Ultimate strength of cracked plate elements under axial compression or tension. . Thin-Walled Structures, , 43(2), 237–272.
Paik, J. K. (2009). Residual ultimate strength of steel plates with longitudinal cracks under axial Compression-Nonlinear finite element method investigations. Ocean Engineering, , 36(3–4), 266–276.
Paik, J. K., Kumar, Y. V. S., & Lee, J. M. (2005). Ultimate strength of cracked plate elements under axial compression or tension. Thin-Walled Structures, , 43(2), 237–272.
Panedpojaman P, P. T. (2010). Effects of tensile softening on the cracking resistance of FRP reinforced concrete under thermal loads. . Struct Eng Mech, 36(4):447–61.
Pantazopoulou SJ, P. K. (2001). Modeling cover-cracking due to reinforcement corrosion in RC structures. . J Eng Mech, 127(4):342–51.
Park, S.-J. P.-K.-G. (2014). Evaluation of residual tensile strength of fire-damaged concrete using a non-linear resonance vibration method. . Magazine of Concrete Research, , 67(5), 235–246.
Paulson, C. R. (2016). Defining yield strength for nonprestressed reinforcing steel. . ACI Structural Journal, , 113(1), 169–178.
Peng, G. F. (2001). Chemical kinetics of C-S-H decomposition in hardened cement paste subjected to elevated temperatures up to 800°C.. Advances in Cement Research, 13(2), 47–52.
Peng, G. F. (2012). Experimental research on fire resistance of reactive powder concrete. Advances in Materials Science and Engineering, 6.
Perras, M. A. (2014). A Review of the Tensile Strength of Rock: Concepts and Testing. . Geotechnical and Geological Engineering, 32(2), 525–546.

Phan, L. T. (1998). Review of mechanical properties of HSC at elevated temperature. Journal of Materials in Civil Engineering, 10(1)(0899-15611), 58-65.
Poh, K. W. (2001). Stress-strain-temperature relationship for structural steel. . Journal of Materials in Civil Engineering, , 13(5), 371–379.
Pothisiri T, P. P. (2012). Modeling of bonding between steel rebar and concrete at elevated temperatures. . Constr Build Mater, 27:130–40.
Pothisiri T, Panedpojaman P. (2012). Modeling of bonding between steel rebar and concrete at elevated temperatures. Constr Build Mater, 27:130–40.
Pothisiri, T. &. (2012). Modeling of bonding between steel rebar and concrete at elevated temperatures. Construction and Building Materials,, 27(1), 130–140.
Pothisiri, T., & Panedpojaman, P. (2013). Modeling of mechanical bond-slip for steel-reinforced concrete under thermal loads. Engineering Structures, 48, 497–507.

Pothisiri, T., & Panedpojaman, P. (2013). Modeling of mechanical bond-slip for steel-reinforced concrete under thermal loads. . Engineering Structures,, 48, 497–507.
Q.Z. Khan, A. A. (2019). Proposed Equation of Elastic Modulus of Hybrid Fibers Reinforced Concrete Cylinders. Technical Journal, University of Engineering and Technology (UET) Taxila, Pakistan,, 1813-1786.
Qiang, X. J. (2016). Mechanical properties and design recommendations of very high strength steel S960 in fire. . Engineering Structures, , 112, 60–70.
Qianmin Ma, R. G. (2015). Mechanical properties of concrete at high temperature—A review. Construction and Building Materials, 93, 371–383.
R. Eligehausen, E. P. (1983). Local bond stress - slip relationships of deformed bars under generalized excitations,. UCB-EERC,.
R. Eligehausen, E.G. Popov, V.V. Bertero,. (1983). Local bond stress - slip relationships of deformed bars under generalized excitations,. UCB-EERC,.
R., T. (1979). Cracking of concrete cover along anchored deformed reinforcing bars. . Mag Concr Res , 31(106):3–12.
Rahal., K. (2017). Shear strength of recycled aggregates concrete. . ScienceDirect. Procedia Engineering ,., 210 (2017) 105–108.
Rekha, K. B. (2016). Residual flexural strength of recycled brick aggregate concrete exposed to high temperatures. . International Journal of Engineering and Technology, , 7(6), 2130–2136.
S. O. Osuji., &. U. (2015). Effects of Elevated Temperature on Compressive Strength of Concrete: A Case Study of Grade 40 Concrete . Nigerian Journal of Technology, 34(3), 472-477.
Saad-Eldeen, S. G. (2012). Effect of corrosion degradationon ultimate strength of steel box girders. . Corrosion Engineering Science and Technology,, 47(4), 272–283.
Samani, A. K. (2012). A stress-strain model for uniaxial and confined concrete under compression. Engineering Structures, 41, 335–349.
Samson Ezekiel, R. S. (2013). Constitutive model for compressive strength and elastic modulus for concrete under elevated temperature. Structures Congress, 10.1061, 2916–2925.
Senthil Kumar, K. &. (2014). Shear strength of concrete with E-waste plastic.Proceedings of the Institution of Civil Engineers . -Construction Materials, , 168(2), 53–56.
Shadafza, E. &. (2016). The Elastic Modulus of Steel Fiber Reinforced Concrete (SFRC) with Random Distribution of Aggregate and Fiber. Civil Engineering Infrastructures Journal, , 49(1), 21–32.
Shah, S. N. (2019). Performance of High Strength Concrete Subjected to Elevated Temperatures: A Review. Fire Technology. Springer New York LLC Fire Technology, 55(10694-018-0791-2), 1571–1597.
Shopov, A. &. (2019). Experimental study of zone of yield strength on corroded construction steel specimens for reuse. MATEC Web of Conferences, , 279, 02009.
Siddique, R. (2011). Utilization of silica fume in concrete: Review of hardened properties. Resources,Conservation and Recycling.
Silva, R. V. (2015). Tensile strength behaviour of recycled aggregate concrete. . Construction and Building Materials,., 83, 108–118.
Solhjoo., R. E. (2007). Characteristic Points of Stress-Strain Curve at High Temperature. International Journal of ISSI, 4 , 24-27.
Suksawang, N. W. (2018). Evaluation of elastic modulus of fiber-reinforced concrete. . ACI Materials Journal,, 115(2), 239–249.
Suksawang, N., Wtaife, S., & Alsabbagh, A. (2018). Evaluation of elastic modulus of fiber-reinforced concrete. . ACI Materials Journal,, 115(2), 239–249.
T. R. Kay, B. R. (1996). Calculation of the heating rate of an unprotected steel member in a standard fire resistance test. Fire Safety Journal, , 26(4):327–350,.
T. Sakthivel, R. G. (2019). Compressive Strength and Elastic Modulus of Concretes with Fly Ash and Slag. J. Inst. Eng. India Ser. A,.
Taghried Isam Mohammed Abdel-Magid. (2017). Quality Evaluation of Steel Reinforcement Bars in Khartoum State. . Red sea university Journal of Basic and Applied Science., 1858 -7658 .
Tao Jin, Y. Y. (2010). Compressive Strength of Self-Compacting Concrete during High-Temperature Exposure. Journal of Materials in Civil Engineering, 22(10), 1005–1011.
Tao, Z. W. (2013). Stress-strain curves of structural and reinforcing steels after exposure to elevated temperatures. Journal of Materials in Civil Engineering,, 25(9), 1306–1316.
Topçu, I. B. (2008.). Properties of reinforced concrete steel rebars exposed to high temperatures. Advances in Materials Science and Engineering, .
Tung, N. &. (2015). Post-peak behavior of concrete specimens undergoing deformation localization in uniaxial compression. Construction and Building Materials, , 99, 109–117.
Uttam B. Kalwane, Y. M. (2016). Shear strength of polymer modified steel fiber reinforced concrete. . Indian Concrete Journal, Vol. 90, Issue 00, pp. 00-00.
V.K.R. Kodur, T. W. (2004). Predicting the fire resistance behavior of high strength concrete columns. Cement & Concrete Composites, 26, 141-153.
Wang X, L. X. (2003). A strain-softening model for steel-concrete bond. . Cem Concr Res , 33:1669–73.
Wang X, Liu X. (2003). A strain-softening model for steel–concrete bond. Cem Concr Res, 33:1669–73.
Wang, J. C. (2016). Experimental study on Bond slip relationship of Steel sleeve. . MATEC Web of Conferences, , 63, 03012.
Wang, J. C., Zhou, J. H., Pan, M. X., & Zhang, D. Y. (2016). Experimental study on Bond slip relationship of Steel sleeve. . MATEC Web of Conferences, , 63, 03012.
Wang, X. Q. (2014). Stress-strain model of austenitic stainless steel after exposure to elevated temperatures. Journal of Constructional Steel Research,, 99, 129–139.
Wenzhong Zheng, H. L. (2012). Compressive behaviour of hybrid fiber-reinforced reactive powder concrete. Materials and Design , 41, 403–409.
Xiao Y, W. H. (n.d.). Compressive behavior of concrete confined by carbon fiber composite jackets. J Mater Civ Eng ASCE2000; , 12(2): 139 –46.

Xiao, J. &. (2004). Study on concrete at high temperature in China - An overview. Fire Safety Journal, 39(1)(10.1016/S0379-7112(03)00093-6), 89–103.
Xiao, J. e. (2019). Strengthening-softening transition in yield strength of nanotwinned Cu. Scripta Materialia,, 162, 372–376.
Xiao, J. X. (2018). Study on high-performance concrete at high temperatures in China (2004–2016) - An updated overview. . Fire Safety Journal.
Xie, F. Y. (2018). Study on Composite Elastic Modulus of Elevated Temperature Diffusion Self-lubricating Material. In IOP Conference Series: . Materials Science and Engineering , 452). .
Youssef, M. A. (2007). General stress-strain relationship for concrete at elevated temperatures. . Engineering Structures, , 29(10), 2618–2634.
Yüzer, N. A. (2004). Compressive strength-color change relation in mortars at high temperature. .Cement and Concrete Research, 34(10), 1803–1807.
ZHAO Shunbo, Z. M. (2019). Study on complete stress-strain curve of steel fiber reinforced lightweight aggregate concrete under uniaxial compression. Journal of Building Structures, .05.019.
Zhao, W. &. (2018). Theoretical model for the bond–slip relationship between ribbed steel bars and confined concrete. Structural Concrete,, 19(2), 548–558.
Zhao, Y. H. (2009). Influence of specimen dimensions and strain measurement methods on tensile stress-strain curves. . Materials Science and Engineering , 525(1–2), 68–77.
Zhongwei Li, M. P. (2017). Ultimate strength of steel beam columns under axial compression. . J Engineering for the Maritime Environment, 1–16 .
Zhou, Y. X. (2018). Mechanical Properties of Hybrid Ultra-High Performance Engineered Cementitous Composites Incorporating Steel and Polyethylene Fibers. . Materials, 11(8), 1448.